

***Nuclear Physics with polarized γ rays
between 2 and 160 MeV***

Henry R. Weller

Duke University and Triangle Universities Nuclear Laboratory

HI γ S PROGRAM

HI γ S

Nearly Mono-energetic γ -rays from 2 to 160 MeV

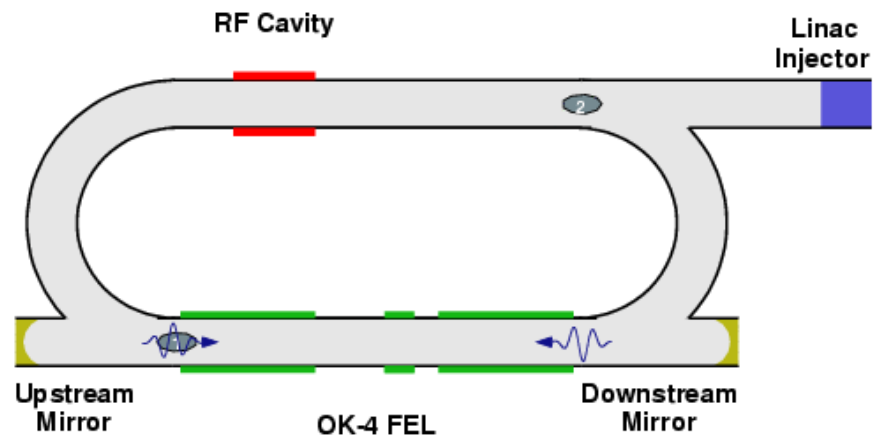
- ***Up to 100 MeV now***
- ***Up to ~160 MeV by 2012***

~100% Linearly and Circularly Polarized γ -rays

High Beam Intensities

(Ran with 2×10^8 on target at 15 MeV -June 2009)

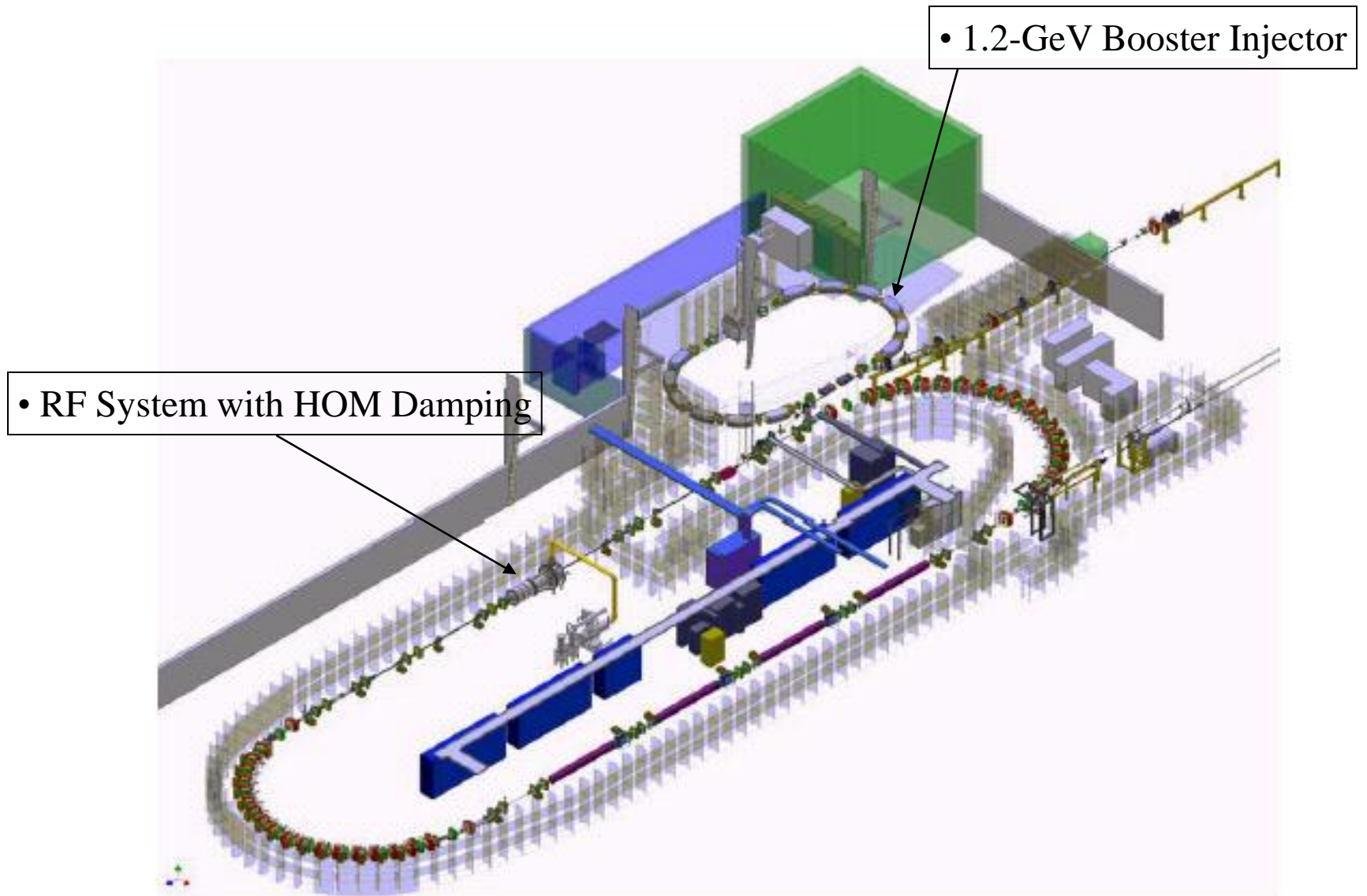
Two Bunch Mode



Created by Brent Perdue, 2005

Mumbai talk 2010

The Upgraded HI γ S Facility



Some typical beam intensities

- | <u>E_γ (MeV)</u> | <u>Beam on target ($\Delta E/E = 3\%$)</u> |
|------------------------------------|---|
| 1 - 2 | $2 \times 10^7 \text{ } \gamma/\text{s}$ |
| 8 - 16 | 2×10^8 (total flux of 4×10^9) |
| 20 - 45 | 2×10^7 |
| 50 - 100 | 8×10^6 (will increase by x3 in 2011) |
| →160 | 4×10^6 (by 2012) |

The $H\gamma S$ Program

A broad based research program in nuclear physics

The program includes studies in the areas of:

Nuclear Astrophysics

Few Body photodisintegration

Nuclear Structure (primarily using NRF)

GDH Sum Rule studies

Compton scattering from nucleons and nuclei

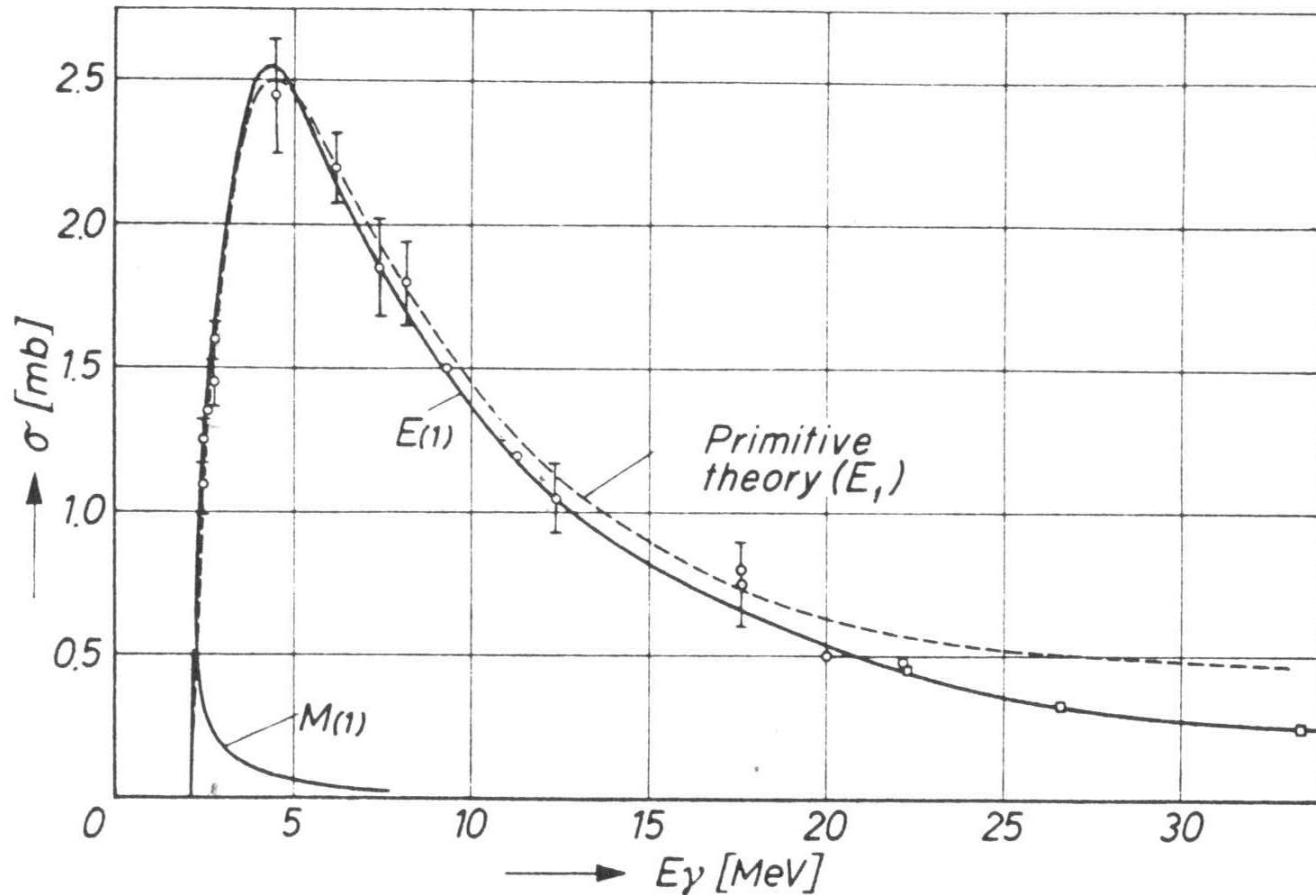
Pion threshold studies

Applications of nuclear physics

Photodisintegration of the deuteron

The E1 gammas are absorbed on the 1^+ (3S_1) state, exciting 0^- , 1^- , and 2^- strength, which then decays into $n+p$ having $S=1$ (since $\Delta S=0$) and $l=1$ (p-waves).

There are 3 different p-wave terms corresponding to $J=0^-$, 1^- , and 2^- . No information about the splittings of these has been available—until now.



d(γ ,n)p at 14 and 16 MeV

(Dissertation topic of Dr. Matthew Blackston)

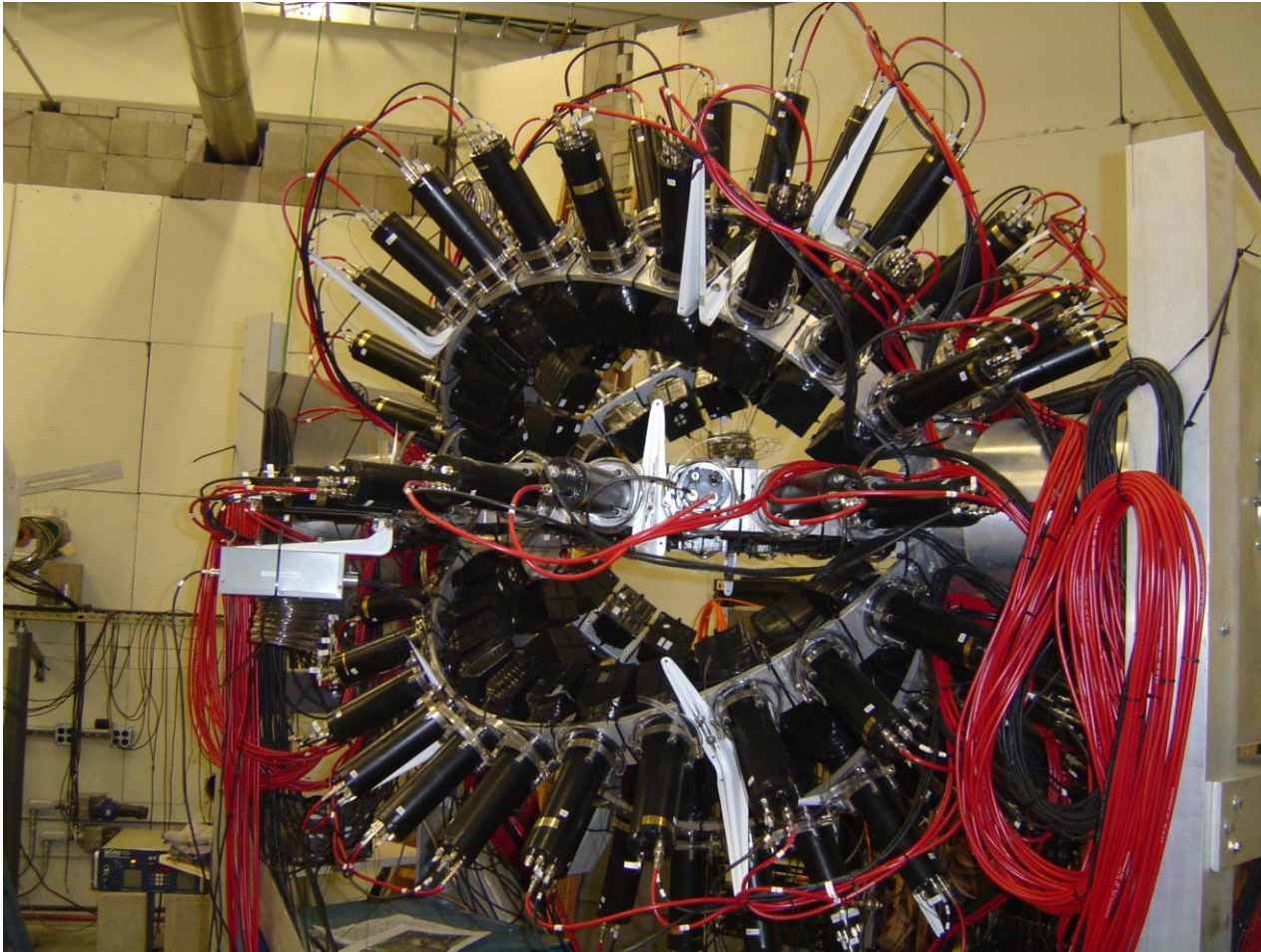
Used the 88 neutron detector array Blowfish (had TOF and PSD).

Heavy water target.

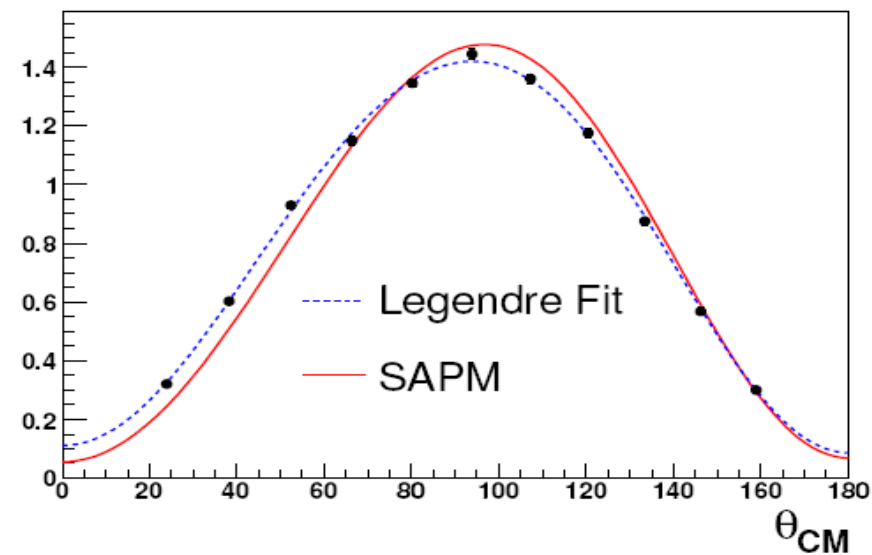
100% linearly polarized beams.

A full simulation was performed using Geant4 to correct the data for finite geometry and multiple scattering effects.

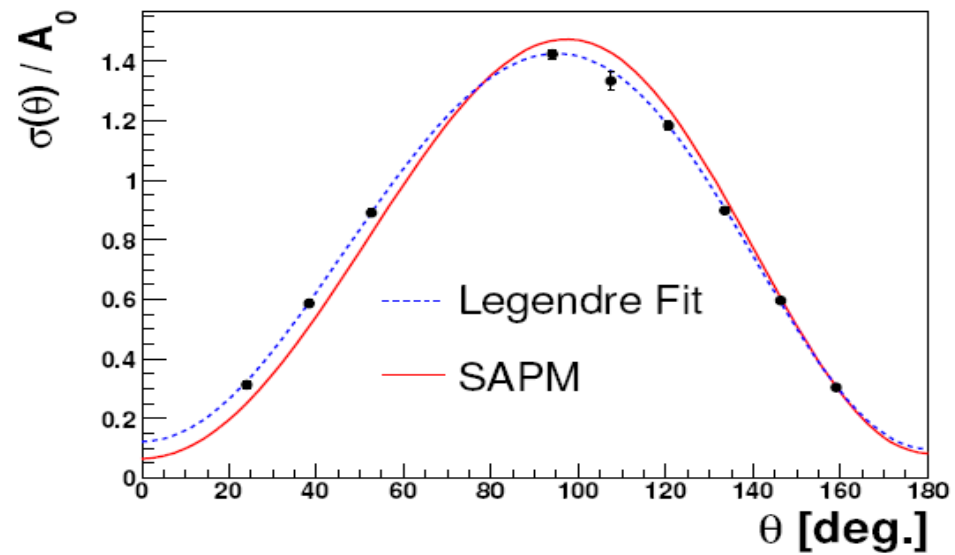
The upgraded *BLOWFISH* array



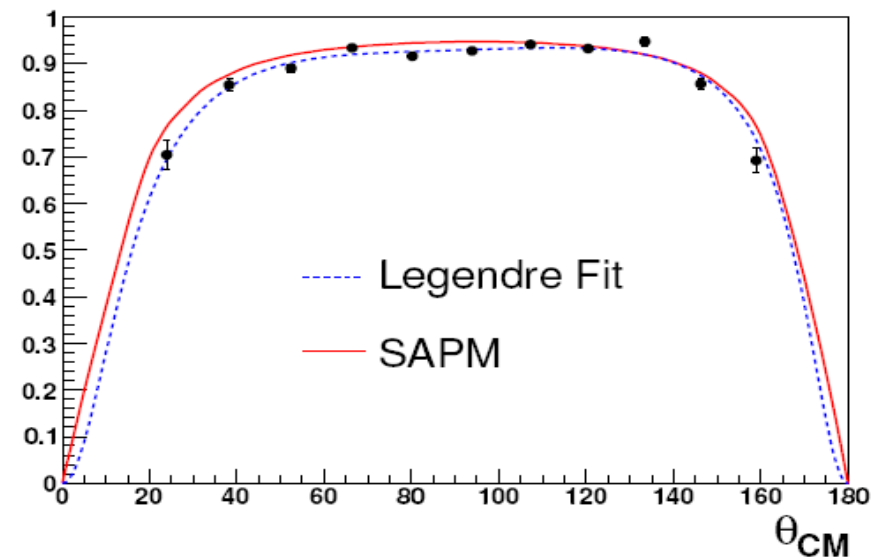
Mumbai talk 2010



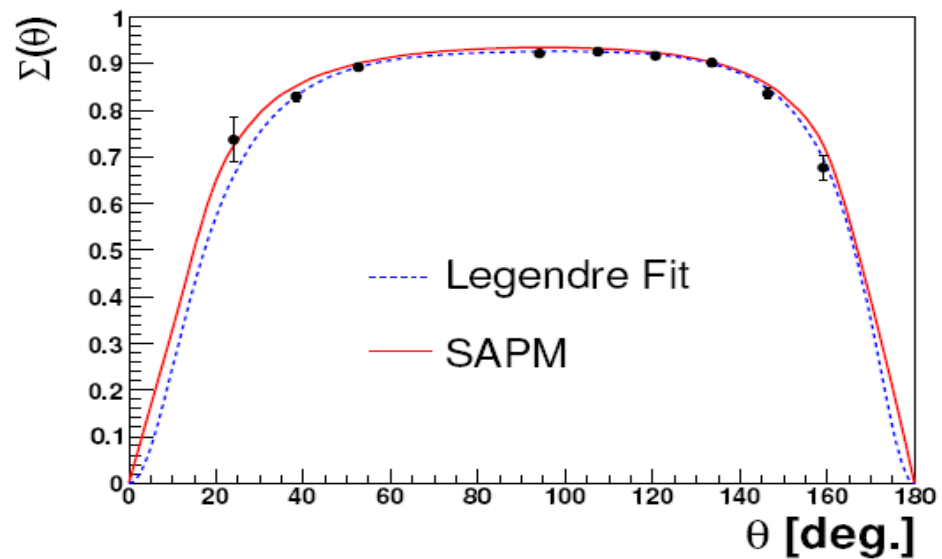
(a) 14 MeV Unpolarized Cross Section.



(b) 16 MeV Unpolarized Cross Section.



(c) 14 MeV Analyzing Power.



(d) 16 MeV Analyzing Power.

- Expansion of $\sigma(\theta)$ and $\Sigma(\theta)$ in Terms of Legendre Polynomials

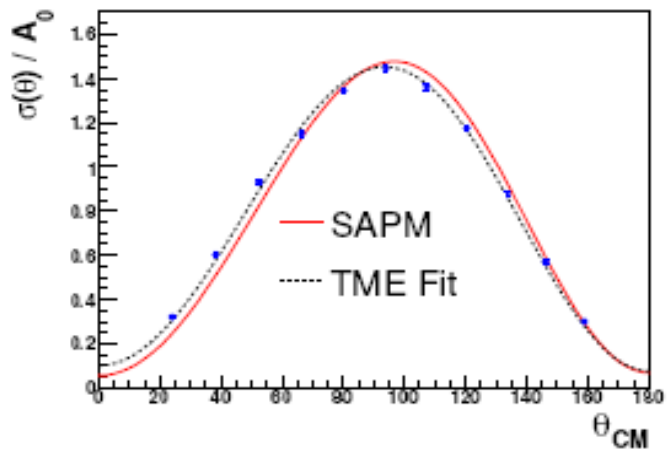
$$\sigma(\theta) = a_0 \left[1 + \sum_{k=1} a_k P_k(\cos \theta) \right] \quad \Sigma(\theta)\sigma(\theta) = \sum_{k=2} e_k P_k^2(\cos \theta)$$

- Using the Formalism of Weller *et al.*², a_k 's and e_k 's can be expanded in terms of amplitudes and relative phases of the Reduced Transition Matrix Elements (TMEs)

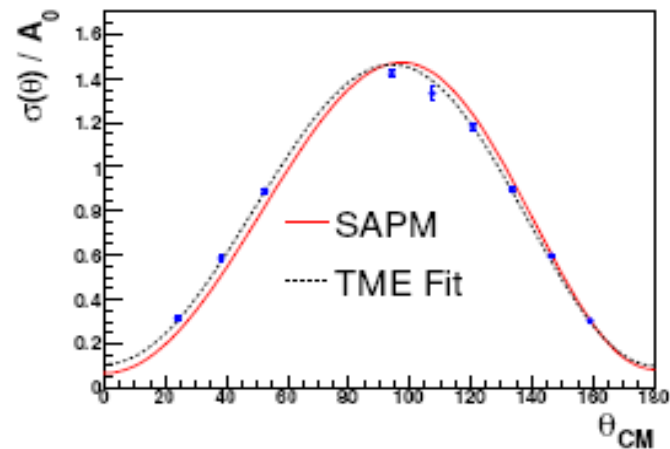
$$\begin{aligned}
A_0 &= 0.25 |^1s_0(M1)|^2 + 0.25 |^3p_0(E1)|^2 + 0.75 |^3p_1(E1)|^2 & (A.1) \\
&+ 1.25 |^3p_2(E1)|^2 + 0.75 |^3d_1(E2)|^2 + 1.25 |^3d_2(E2)|^2 \\
&+ 1.75 |^3d_3(E2)|^2
\end{aligned}$$

$$\begin{aligned}
a_1 &= 0.866 |^3p_0(E1)| |^3d_1(E2)| \cos(\delta_{^3p_0} - \delta_{^3d_1}) & (A.2) \\
&+ 0.649 |^3p_1(E1)| |^3d_1(E2)| \cos(\delta_{^3p_1} - \delta_{^3d_1}) \\
&+ 1.949 |^3p_1(E1)| |^3d_2(E2)| \cos(\delta_{^3p_1} - \delta_{^3d_2}) \\
&+ 0.043 |^3p_2(E1)| |^3d_1(E2)| \cos(\delta_{^3p_2} - \delta_{^3d_1}) \\
&+ 0.649 |^3d_2(E2)| |^3p_2(E1)| \cos(\delta_{^3d_2} - \delta_{^3p_2}) \\
&+ 3.637 |^3p_2(E1)| |^3d_3(E2)| \cos(\delta_{^3p_2} - \delta_{^3d_3})
\end{aligned}$$

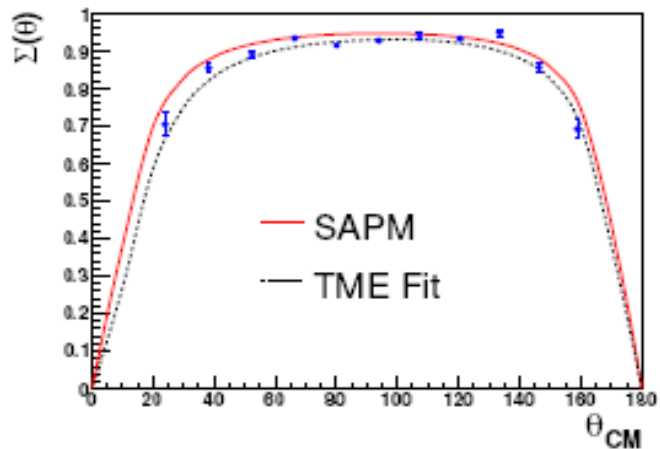
$$\begin{aligned}
a_2 &= -0.187 |^3p_1(E1)|^2 & (A.3) \\
&- 0.438 |^3p_2(E1)|^2 + 0.187 |^3d_1(E2)|^2 \\
&+ 0.223 |^3d_2(E2)|^2 + 0.857 |^3d_3(E2)|^2 \\
&- 0.500 |^3p_0(E1)| |^3p_2(E1)| \cos(\delta_{^3p_0} - \delta_{^3p_2}) \\
&- 1.125 |^3p_1(E1)| |^3p_2(E1)| \cos(\delta_{^3p_1} - \delta_{^3p_2}) \\
&+ 0.625 |^3d_1(E2)| |^3d_2(E2)| \cos(\delta_{^3d_1} - \delta_{^3d_2}) \\
&+ 0.071 |^3d_1(E2)| |^3d_3(E2)| \cos(\delta_{^3d_1} - \delta_{^3d_3}) \\
&+ 0.714 |^3d_2(E2)| |^3d_3(E2)| \cos(\delta_{^3d_2} - \delta_{^3d_3})
\end{aligned}$$



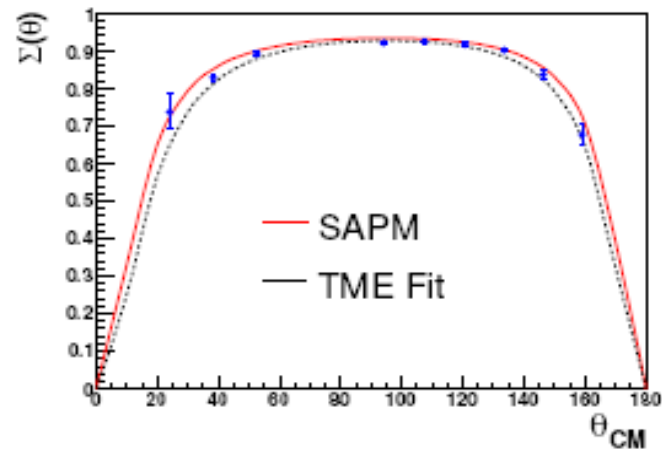
(a) 14 MeV Unpolarized Cross Section.



(b) 16 MeV Unpolarized Cross Section.



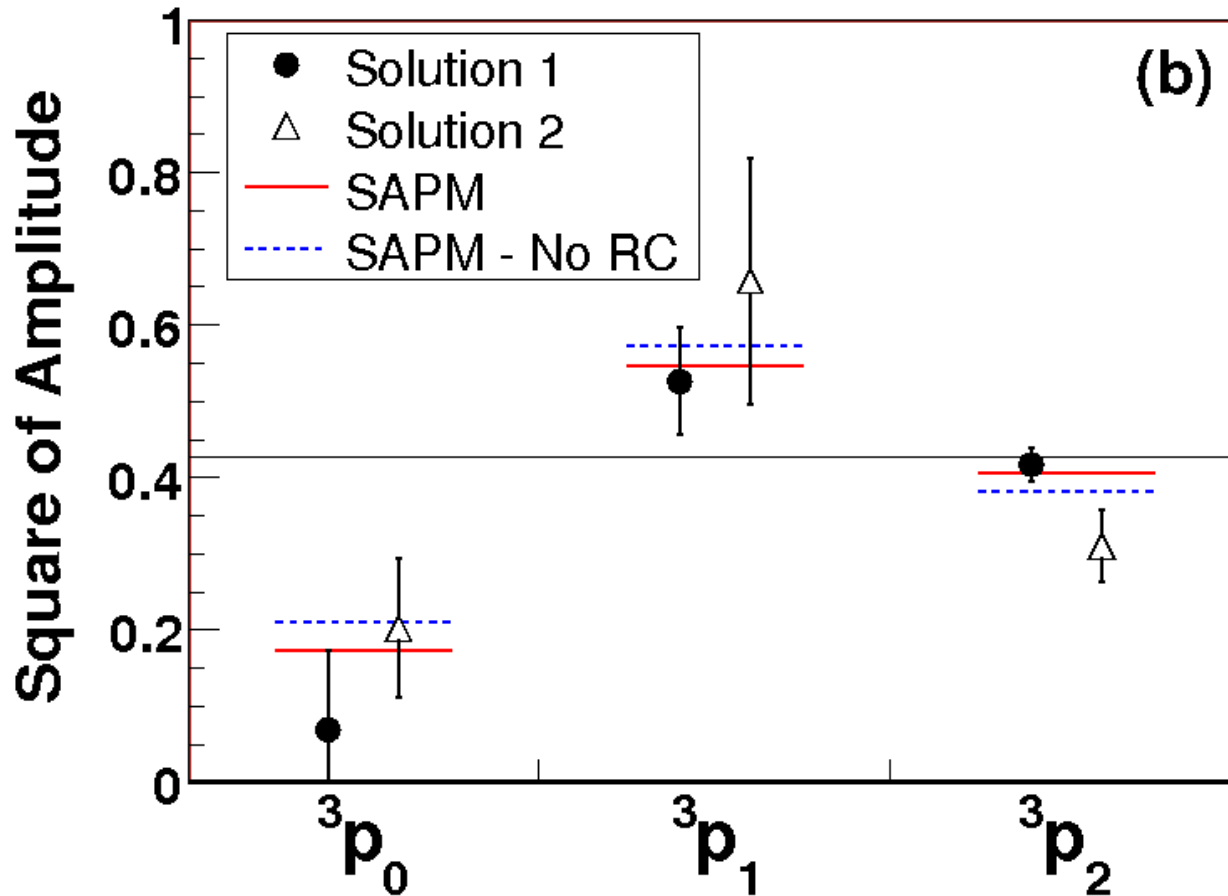
(c) 14 MeV Analyzing Power.



(d) 16 MeV Analyzing Power.

Figure 6.11: Fits to the observables with splittings. The error bars are statistical only. The blue curve is the fit and the red curve is from the SAPM calculation.

- First determination of the splittings in the p-wave (E1) amplitudes in photodisintegration of the deuteron at 16 MeV.



GDH Sum Rule studies @ HI γ S

Measure the GDH integrand on d below pion threshold.

- ***Compare to theoretical predictions. Provides extremely sensitive test of spin dependent effects such as relativistic spin-orbit currents.***
- ***Combine with the global effort to measure this for n , p and d . Our piece is essential for a test of consistency and a search for new physics.***

The Gerasimov Drell Hearn Sum Rule

$$\int_{th}^{\infty} (\sigma_P - \sigma_A) dE / E = \frac{4\pi^2 \alpha}{m^2} \kappa^2 S = I_{GDH}$$

The Gerasimov-Drell-Hearn (GDH) Sum Rule for Deuteron

The GDH Integral

$$I^{\text{GDH}} = \int_{2.2 \text{ MeV}}^{\infty} (\sigma_{\text{P}}(E) - \sigma_{\text{A}}(E)) \frac{dE}{E} = 4 \pi^2 \kappa^2 \frac{e^2}{M^2}$$

$$\vec{M} = (Q + \kappa) \frac{e}{M} \vec{S};$$

$\sigma_{\text{P/A}}(E)$ are the total cross sections for the absorption of circularly polarized photons on a target with spin Parallel/Antiparallel to the spin of the photon;

κ = anomalous magnetic moment (of the deuteron).

$$\kappa_{\text{d}} = -0.143 \mu_{\text{m}}$$

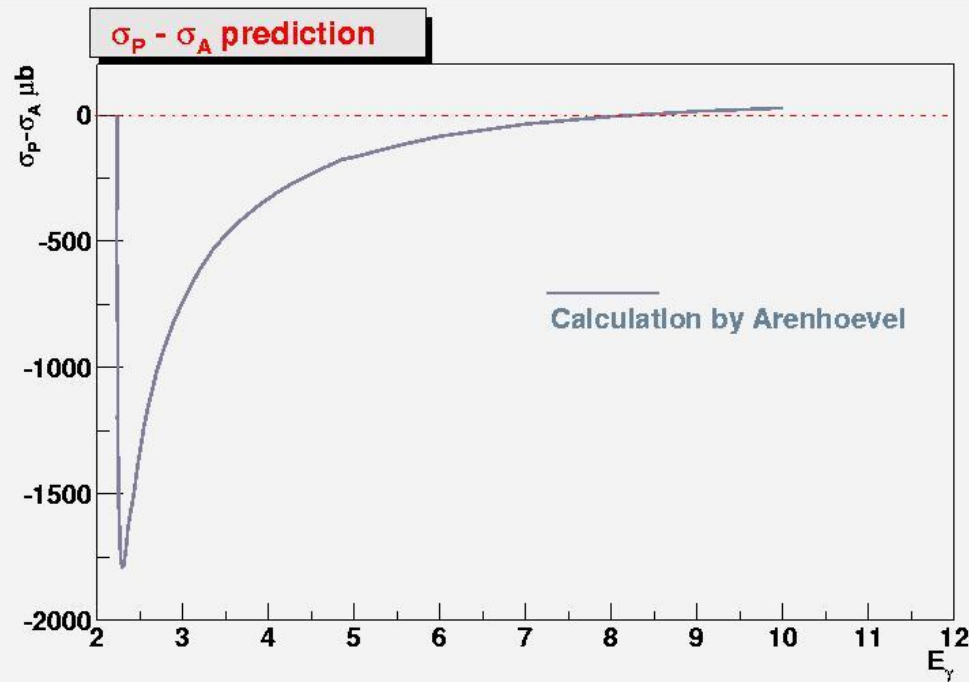
→ $I^{\text{GDH}} \text{ Predicted} = 0.65 \mu\text{b}$

$$I^{\text{GDH}}_{\text{total}} = \int_{2.2 \text{ MeV}}^{E_{\pi}} \dots + \int_{E_{\pi}}^{\infty} \dots$$

E_{π} = pion production threshold

$$\int_{E_{\pi}}^{\infty} = \int (\text{proton}) + \int (\text{neutron}) = 436 \mu\text{b}$$

$$\int_{2.2 \text{ MeV}}^{E_{\pi}} \dots \approx -436 \mu\text{b}$$



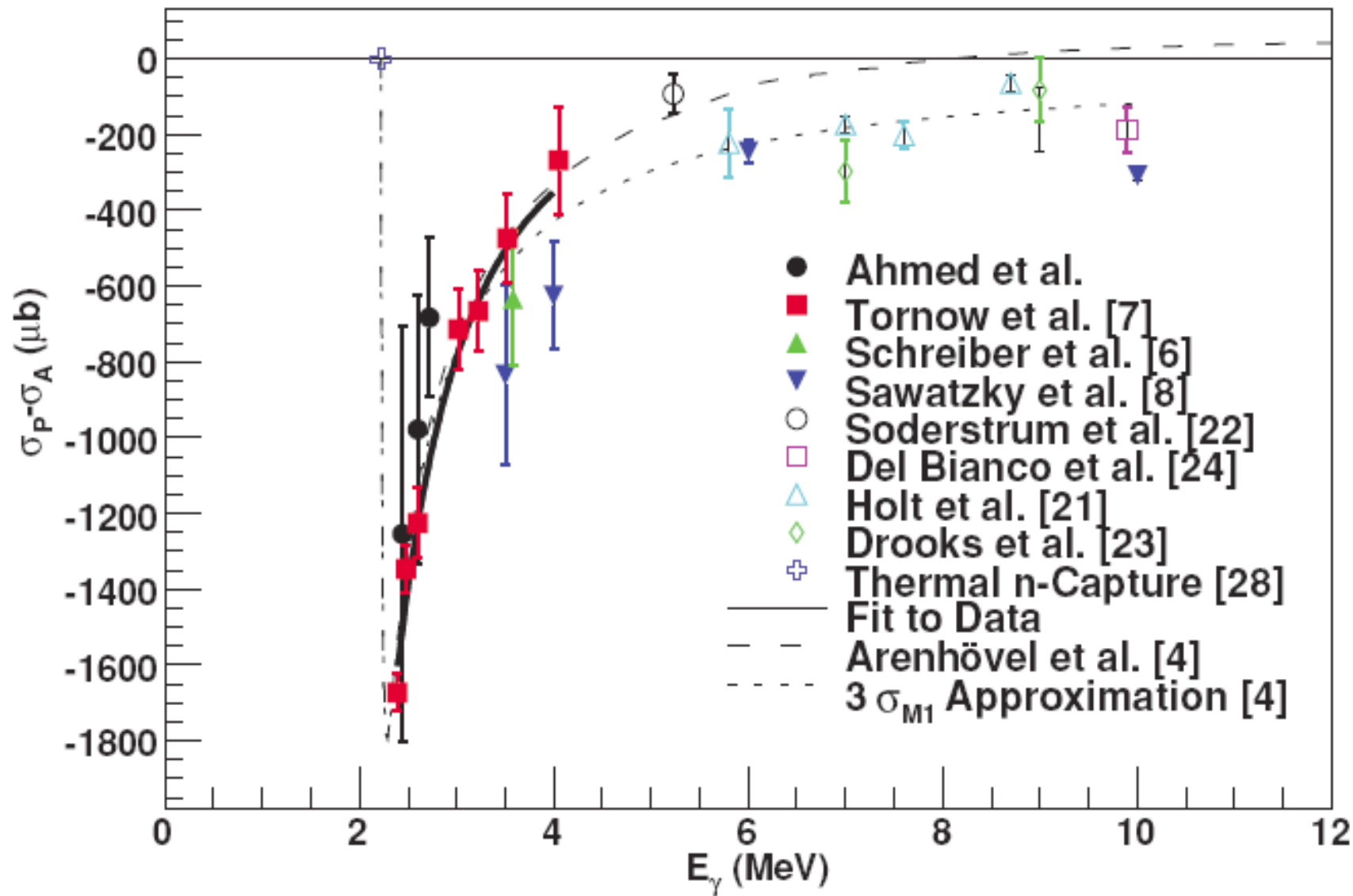
The GDH integrand can be written in terms of the contributing T-matrix elements

[if no p or d-wave splitting, $\sigma_P - \sigma_A = -3 \sigma(M1)$]

$$\begin{aligned} \sigma_P - \sigma_A = \frac{\pi \lambda^2}{2} & \left[- |M1(^1S_0)|^2 - |E1(^3P_0)|^2 \right. \\ & - \frac{3}{2} |E1(^3P_1)|^2 + \frac{5}{2} |E1(^3P_2)|^2 - \frac{3}{2} |E2(^3D_1)|^2 \\ & \left. - \frac{5}{6} |E2(^3D_2)|^2 + \frac{7}{3} |E2(^3D_3)|^2 \right], \end{aligned} \quad (9)$$

At very low energies, s-waves will dominate. If p and d-waves are present but don't split, their contributions drop out.

$$\begin{aligned}\sigma_P - \sigma_A &= \frac{\pi\lambda^2}{2} [-|M1(^1S_0)|^2] \\ &= -3\sigma(M1).\end{aligned}$$



Results for the GDH integral at low energies

The solid black curve was a fit to the data using a Lorentzian line shape parameterized by amplitude, centroid and width. The GDH integral of this function up to 6 MeV gave a value of

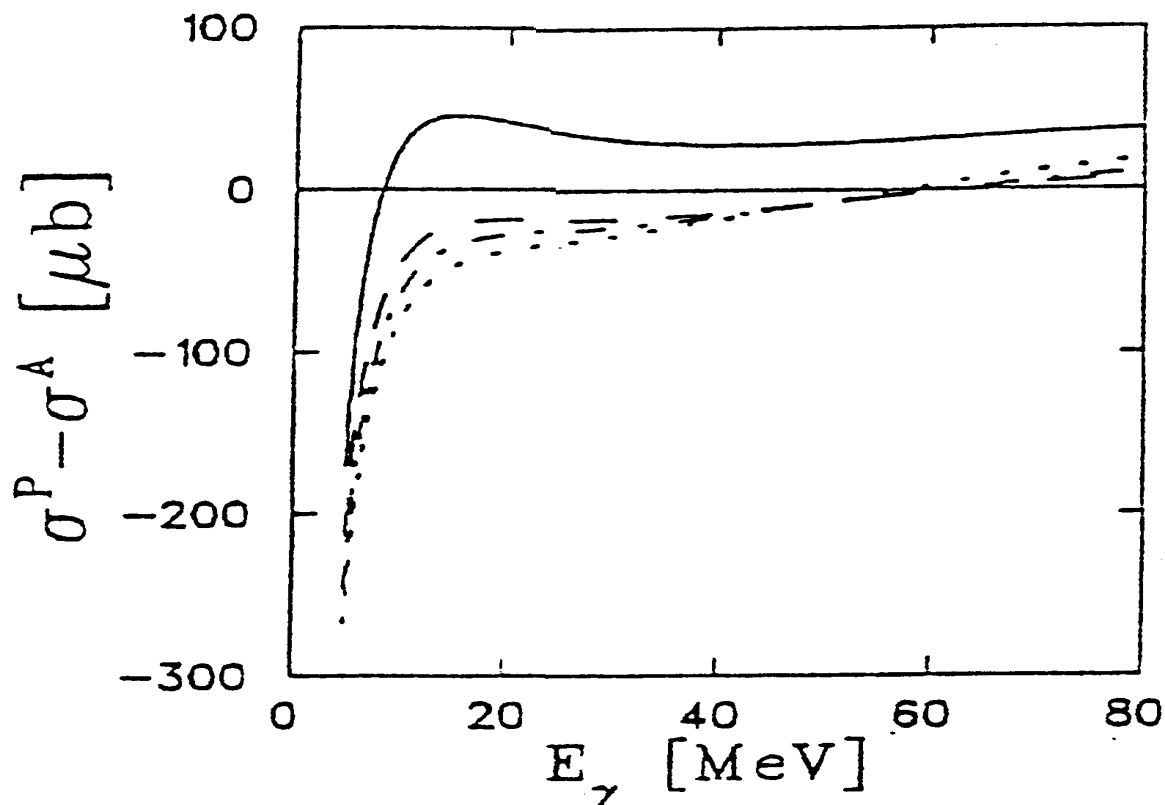
$$\text{GDH (thresh} \rightarrow 6 \text{ MeV)}_{\text{exp}} = \mathbf{-603 \pm 43 \mu\text{b}}$$

(note: already much larger than -436 μb)

Theory (Arenhoevel et al.) gives **-627 μb (full)**

and **-662 μb (s-wave only)**

Predicted behavior (Ahrenhovel) of the GDH integrand. Solid line includes a *relativistic* correction.

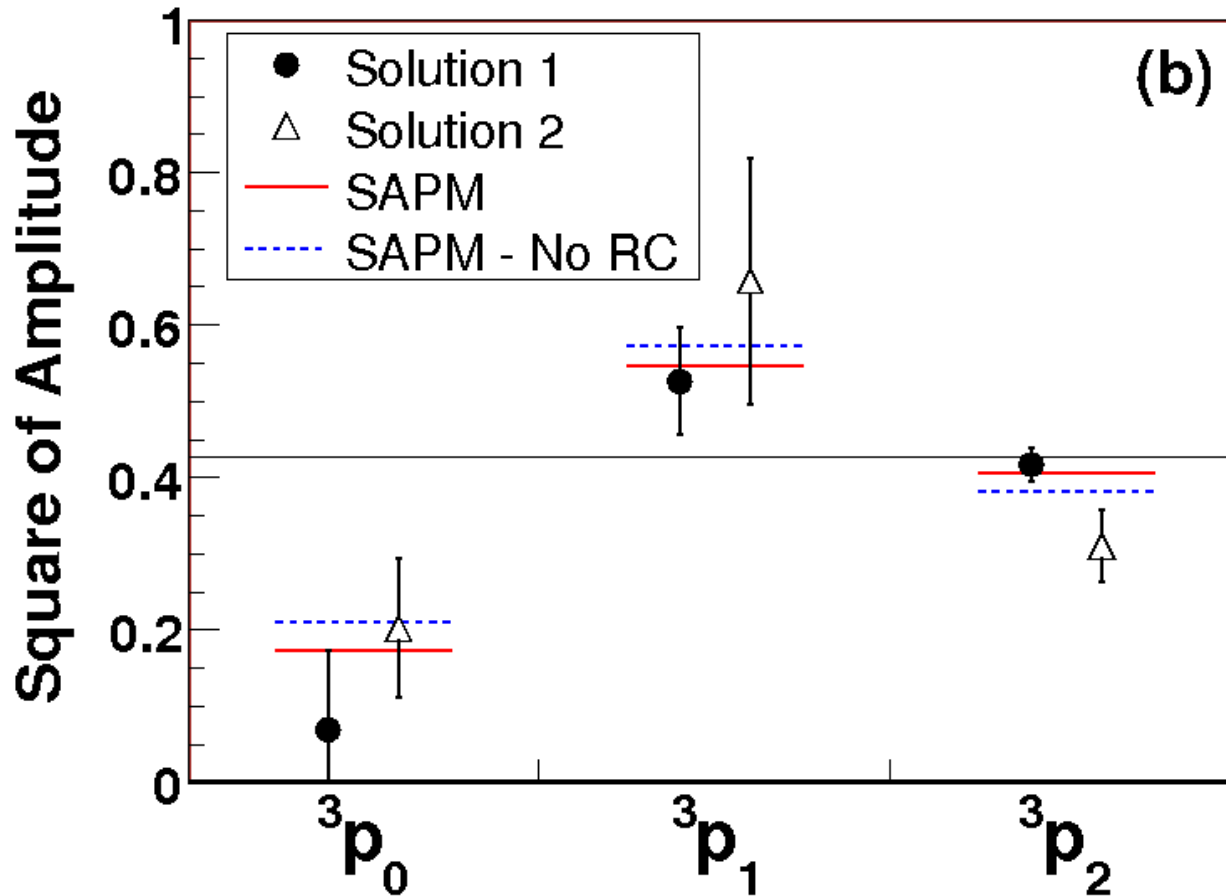


Relativistic contributions

Leading order relativistic contributions are required to give the correct form of the term linear in photon momentum in the low-energy expansion of the Compton amplitude.

The relativistic spin-orbit current effects the splitting of the p-wave amplitudes, leading to a positive value of the GDH integrand. (*It increases the relative strength of the 3p_2 term.*)

- First determination of the splittings in the p-wave (E1) amplitudes in photodisintegration of the deuteron at 16 MeV.

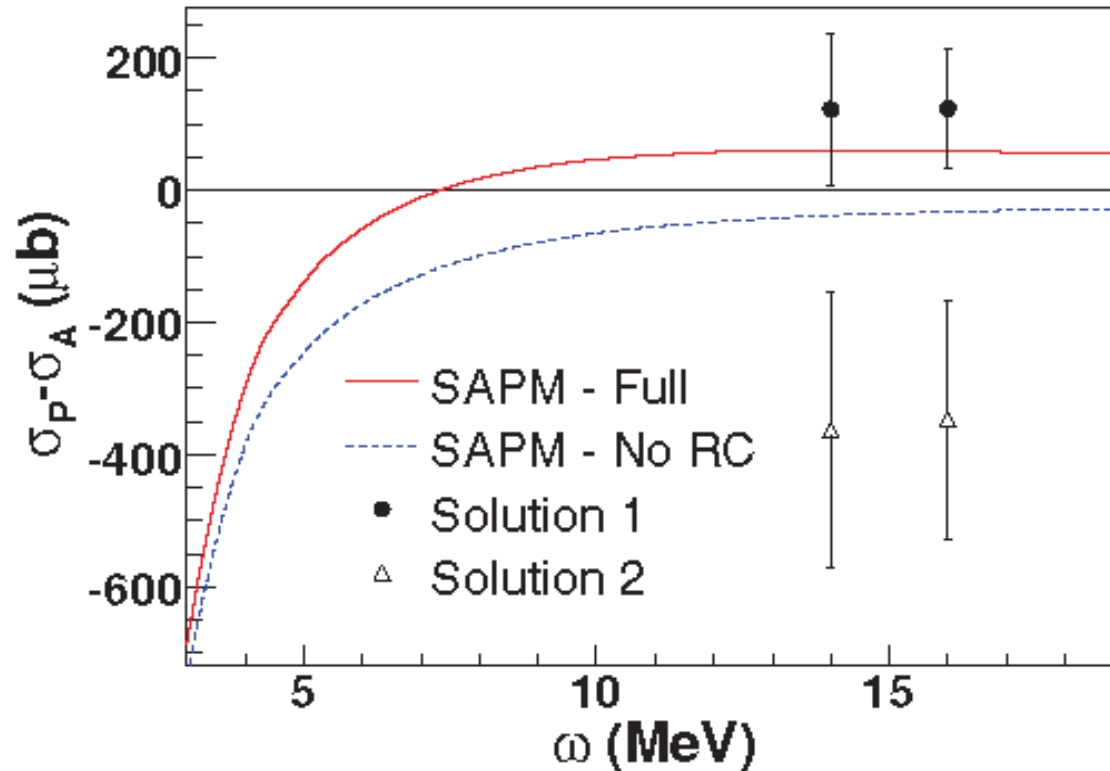


The GDH integrand can be written in terms of the contributing T-matrix elements

[if no p or d-wave splitting, $\sigma_P - \sigma_A = -3 \sigma(M1)$]

$$\begin{aligned} \sigma_P - \sigma_A = \frac{\pi \lambda^2}{2} & \left[- |M1(^1S_0)|^2 - |E1(^3P_0)|^2 \right. \\ & - \frac{3}{2} |E1(^3P_1)|^2 + \frac{5}{2} |E1(^3P_2)|^2 - \frac{3}{2} |E2(^3D_1)|^2 \\ & \left. - \frac{5}{6} |E2(^3D_2)|^2 + \frac{7}{3} |E2(^3D_3)|^2 \right], \end{aligned} \quad (9)$$

Results for the GDH integrand from the two solutions. Without p-wave splittings the value at 14 MeV is predicted to be $-50 \mu\text{b}$ (from the s-wave M1 term). Positive values are predicted only when the relativistic contribution is included.



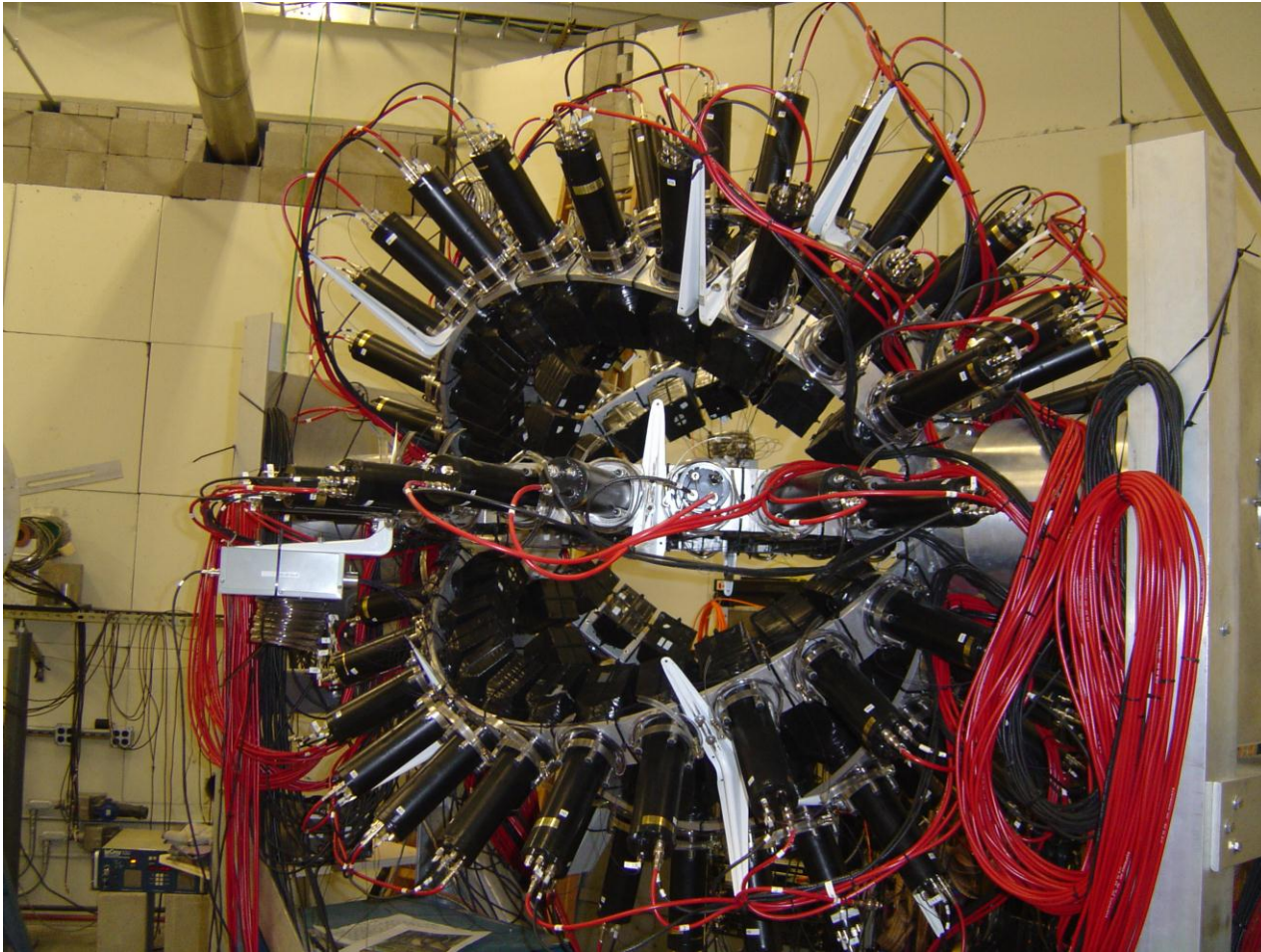
Requirements for direct measurements of
The GDH
integrand on the Deuteron

Circularly Polarized gamma rays—available NOW!

Neutron detection array—Blowfish—ready to go!

Polarized frozen-spin target—Under construction in collaboration with *Don Crabb* and *Blaine Norum* of U. Va. Scheduled to be installed this spring.

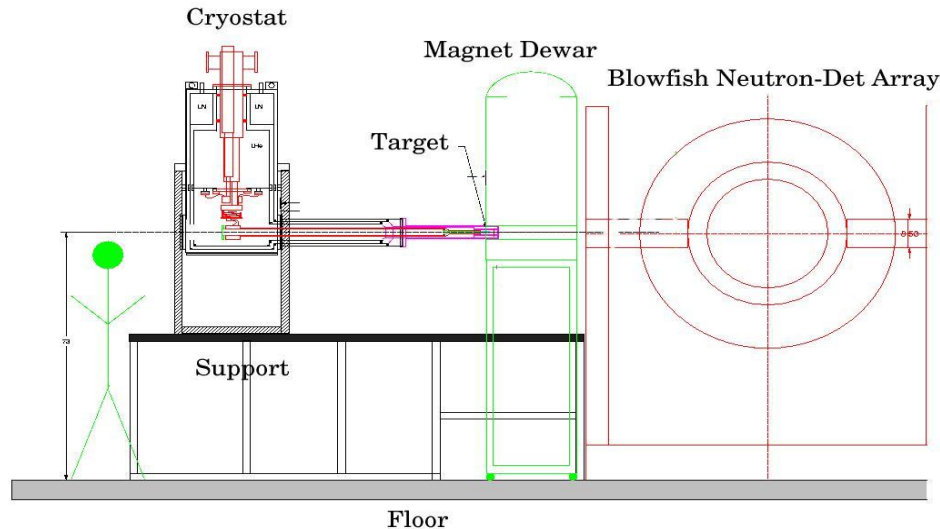
The upgraded *BLOWFISH* array

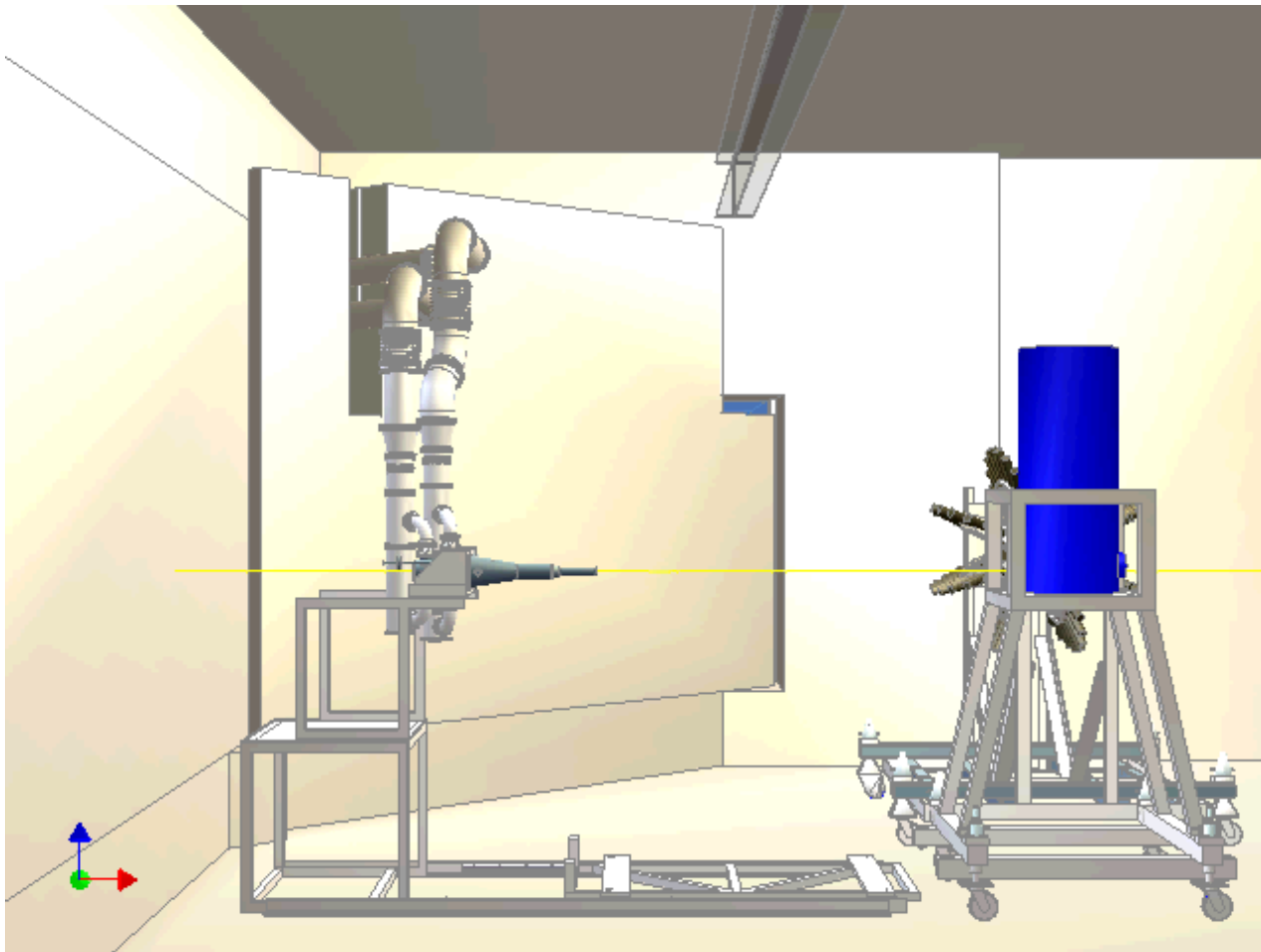


Mumbai talk 2010

Frozen Spin Polarized Deuterium Target --target and installation (loading dock system) are fully funded.

- **Butanol**
- **Polarization ~ 80 %**
- **Polarizing Field ~ 2.5 T**
- **Holding Field ~ 0.6 T**
- Thickness ~ 3.5×10^{23} d/cm²**





Mumbai talk 2010

The GDH integrand for deuterium

A 300 hour run will allow us to measure the GDH integrand between 5 and 50 MeV to an overall accuracy of about 5% or better, assuming a beam of 1×10^7 γ/s with ~5% energy spread.

Besides being a crucial piece of the world's data on the GDH sum rule, the integrand will provide important tests of potential and EFT calculations, being more sensitive to spin physics and relativistic contributions than any previously measured observable.

Anticipated schedule

The HIFROST target will be installed in 2011.

We (the GDH @HI γ S Collaboration) expect to begin taking data in mid 2011, with preliminary results between 5 and 50 MeV by the end of the year.

Conclusions and future studies

Precision data on photodisintegration of the deuteron with 100% linearly polarized beams @HIγS has given us ***the first determination of the splittings of the E1 p-wave amplitudes.***

These results ***confirm the positive value of the GDH integrand which arises theoretically from relativistic spin-orbit currents.***

The results also allow for ***the first determination of the forward spin-polarizability of the deuteron.*** The value deduced is in reasonable agreement with EFT and potential model predictions.

Extension of GDH measurements up to 100 MeV will be performed starting next year.

• **Compton @H γ S**

- ***Study of the fundamental structure of the nucleon:***
- **GOALS:**
- ***Use the intense polarized beams at H γ S to obtain precise values of the electric and magnetic polarizabilities of the proton and the neutron.***
- ***Perform double polarization experiments to obtain precise values of the spin-polarizabilities of the proton and the neutron.***

Start-up experiment--

Want to start up with an experiment which can benchmark our experimental capabilities while taking advantage of the unique features of our beam.

Chose to study ^{209}Bi in the IVGQR region.

High counting rates

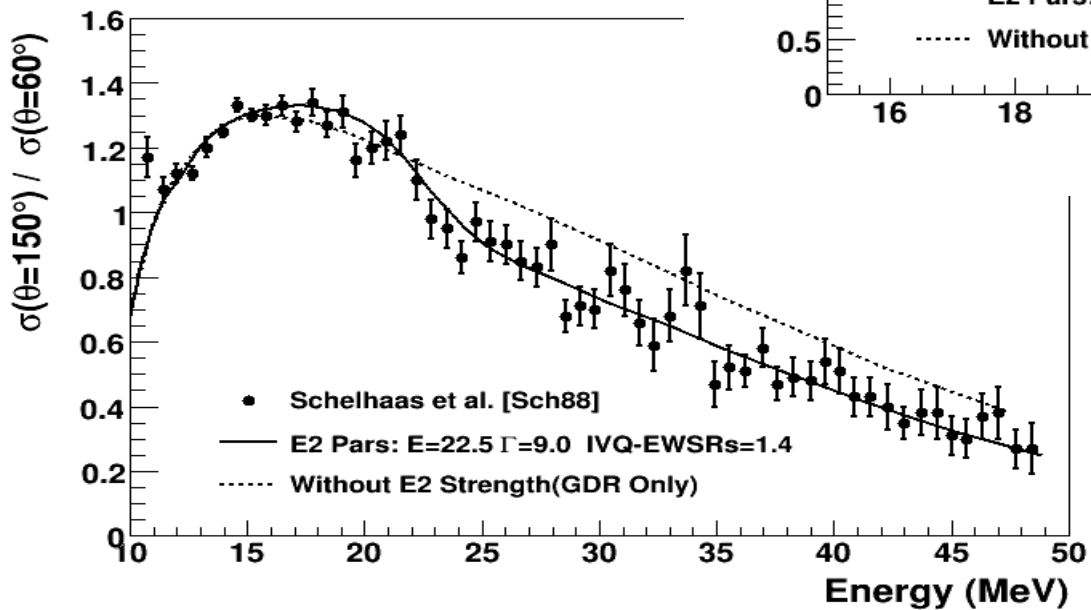
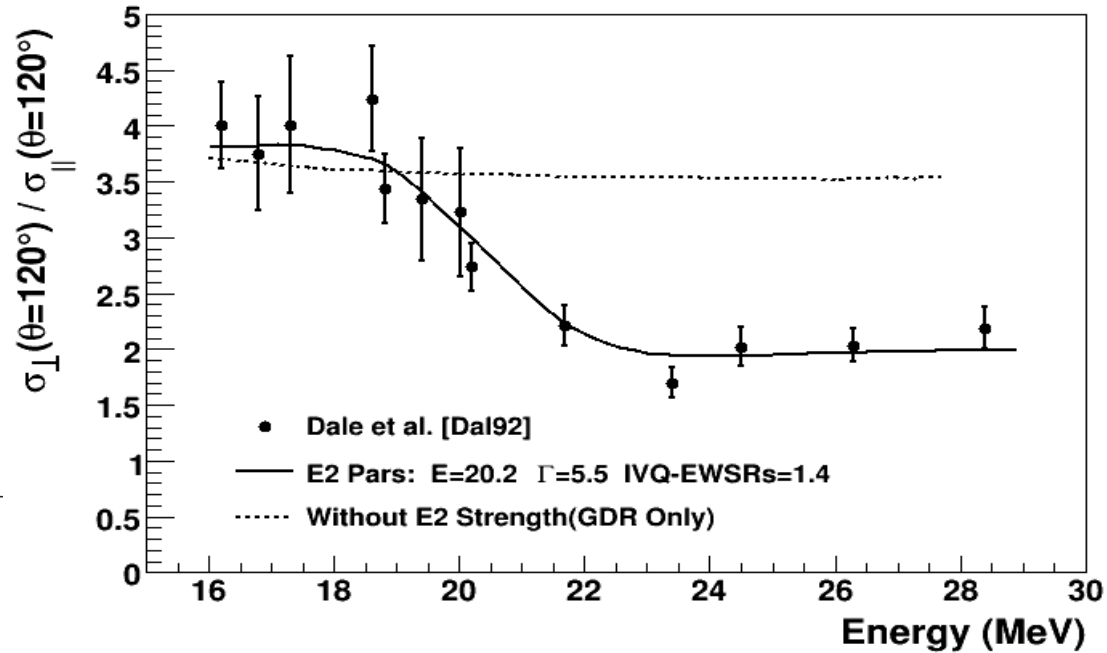
No previous results

Target available

Previous ²⁰⁸Pb(γ,γ) IVGQR Studies

σ_{\perp} • perpendicular to
• polarization plane

σ_{\parallel} • parallel to
• polarization plane



$\sigma(\theta)$: Unpolarized

Scattering Theory

Assumptions: (GDR Dominates)

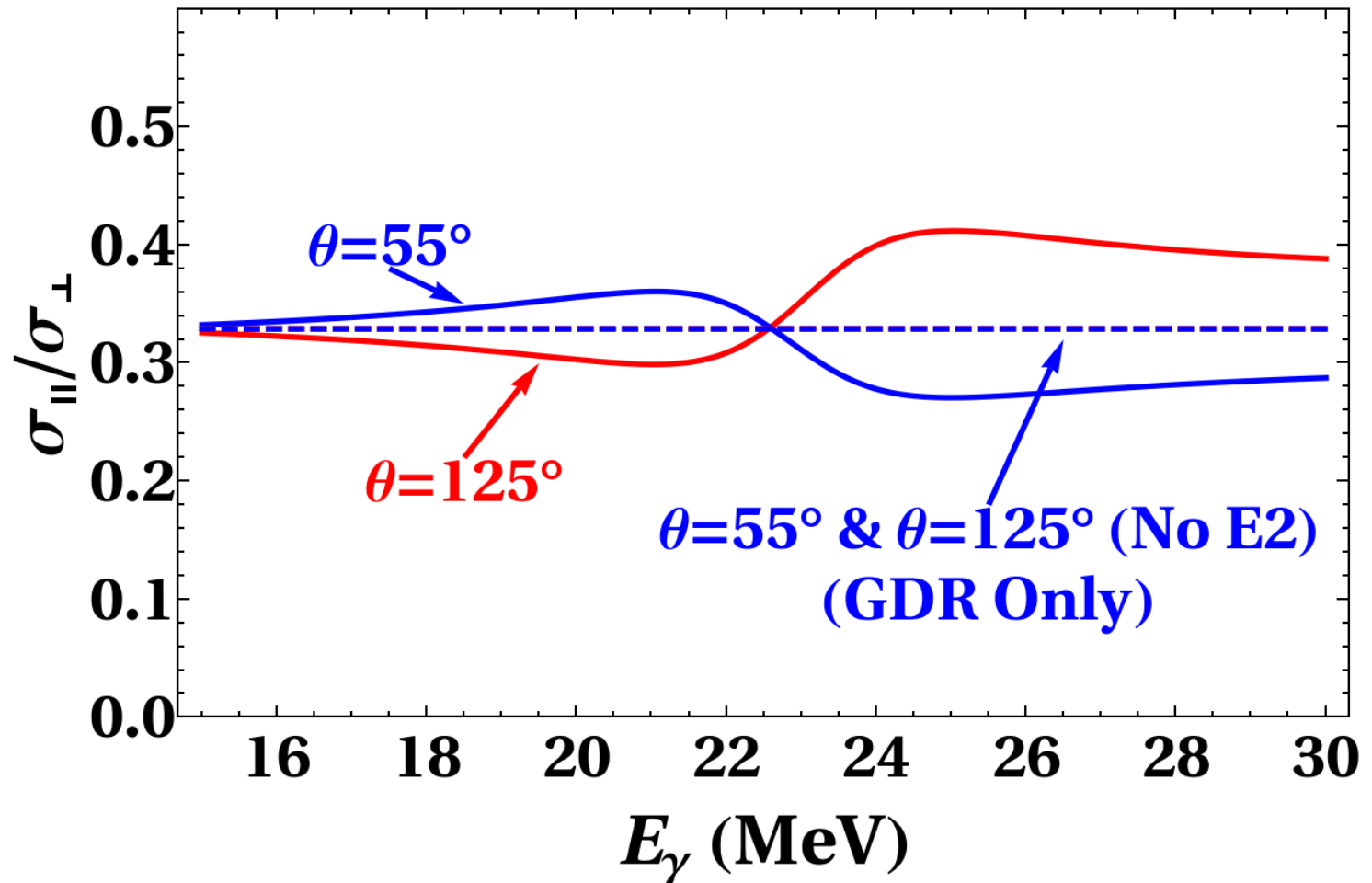
- Modified Thomson Amp included in C^{E1}
- E2 strength due to IVGQR

$$\frac{\sigma_{\parallel}}{\sigma_{\perp}} = \cos^2 \theta + \frac{2|C^{E2}|}{|C^{E1}|} \cos(\phi_{E2} - \phi_{E1}) \left[\cos^3 \theta - \cos \theta \right]$$

$$\cos(\phi_{E2} - \phi_{E1}) \begin{cases} < 0, E < E_{res} \\ > 0, E > E_{res} \end{cases}$$

θ	$\cos^2 \theta$	$\cos^3 \theta - \cos \theta$
125°	0.33	0.38
55°	0.33	-0.38

Polarization Ratio

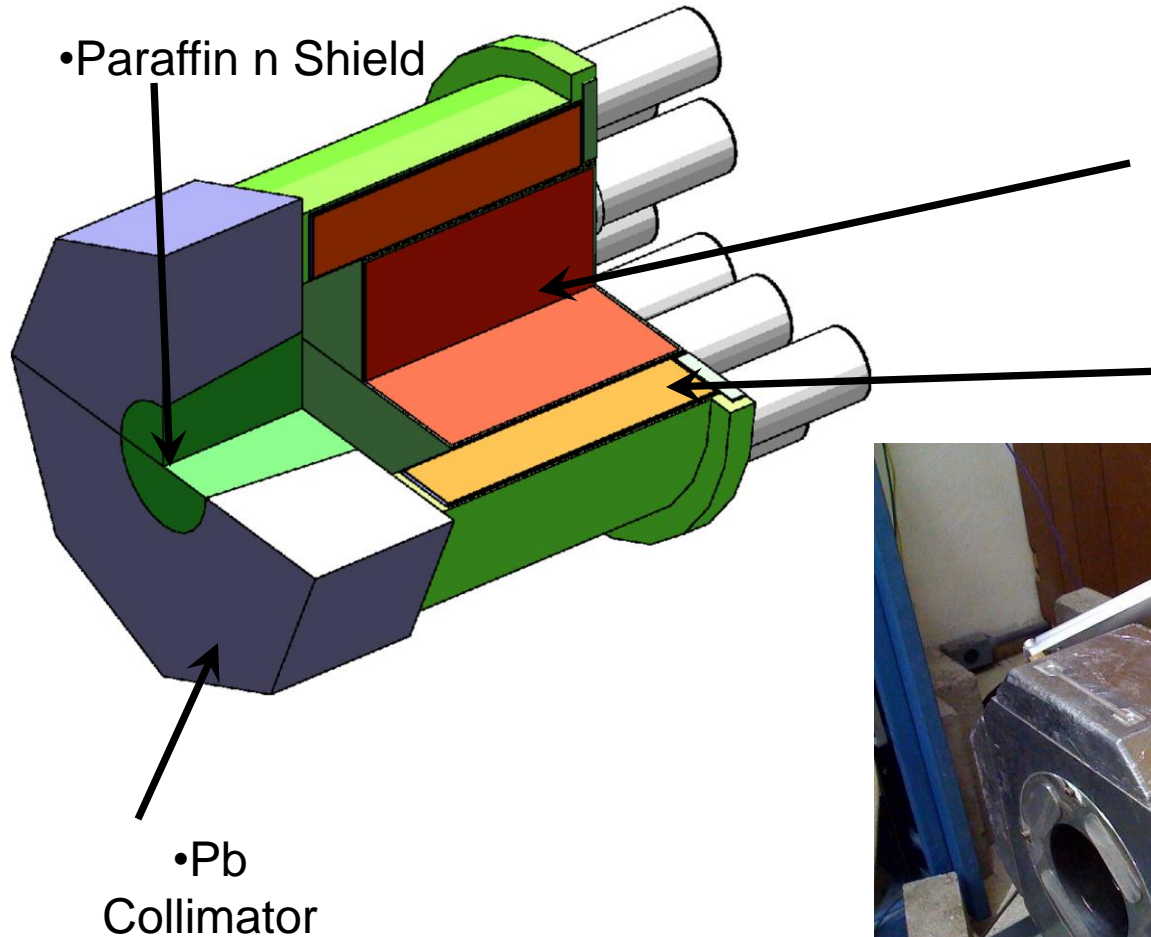


- **The HINDA Array**
(**H γ S NaI Detector Array**)

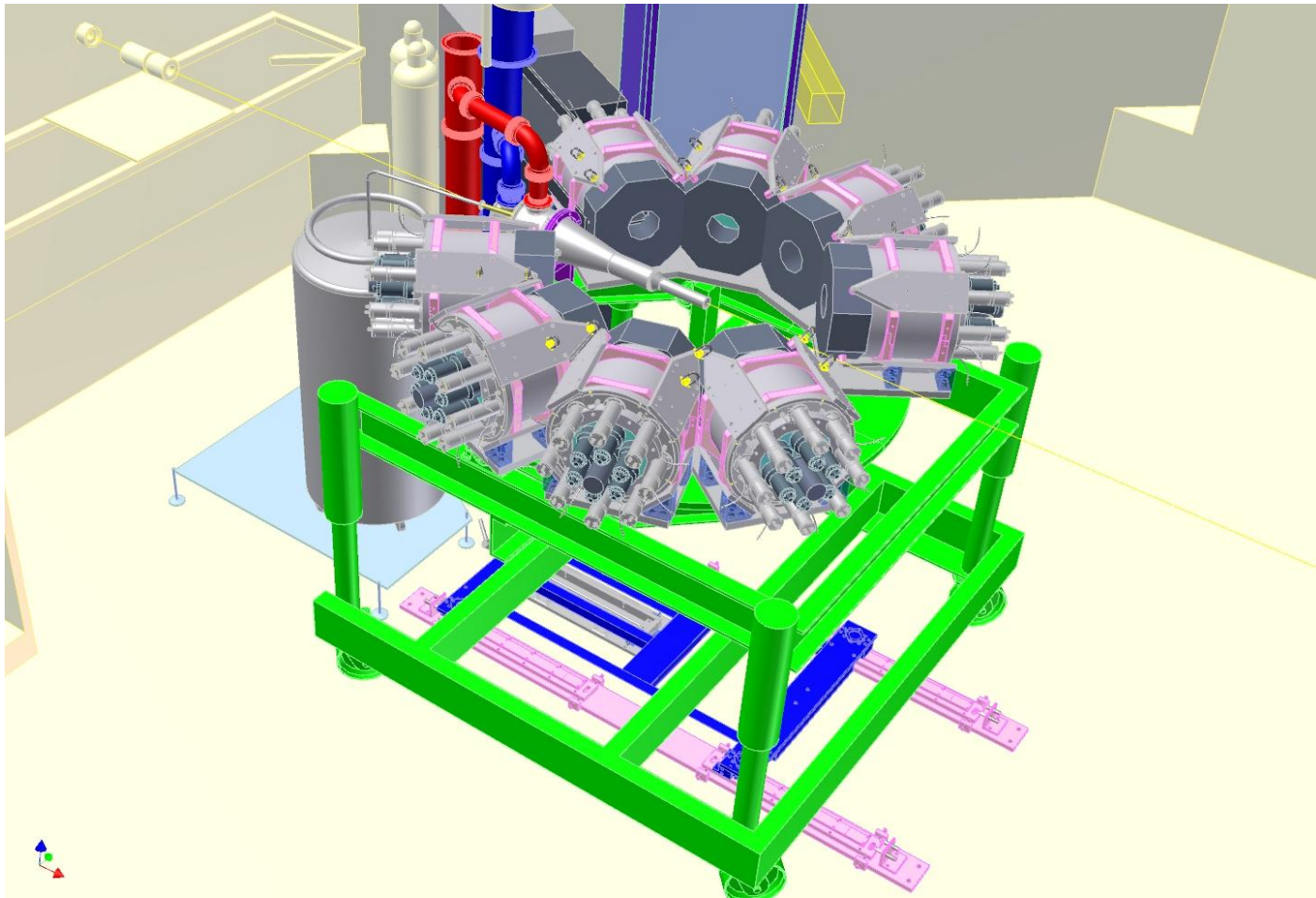
- NSF/MRI funded project—a high resolution-high acceptance gamma-ray spectrometer consisting of eight 10”x12” NaI detectors in 3” thick segmented NaI shields.

- **The Compton@H γ S Collaboration**

•The 8-detector HINDA Array



The HINDA Array @ HIγS



Mumbai talk 2010

HINDA Setup

^{209}Bi Scattering Target

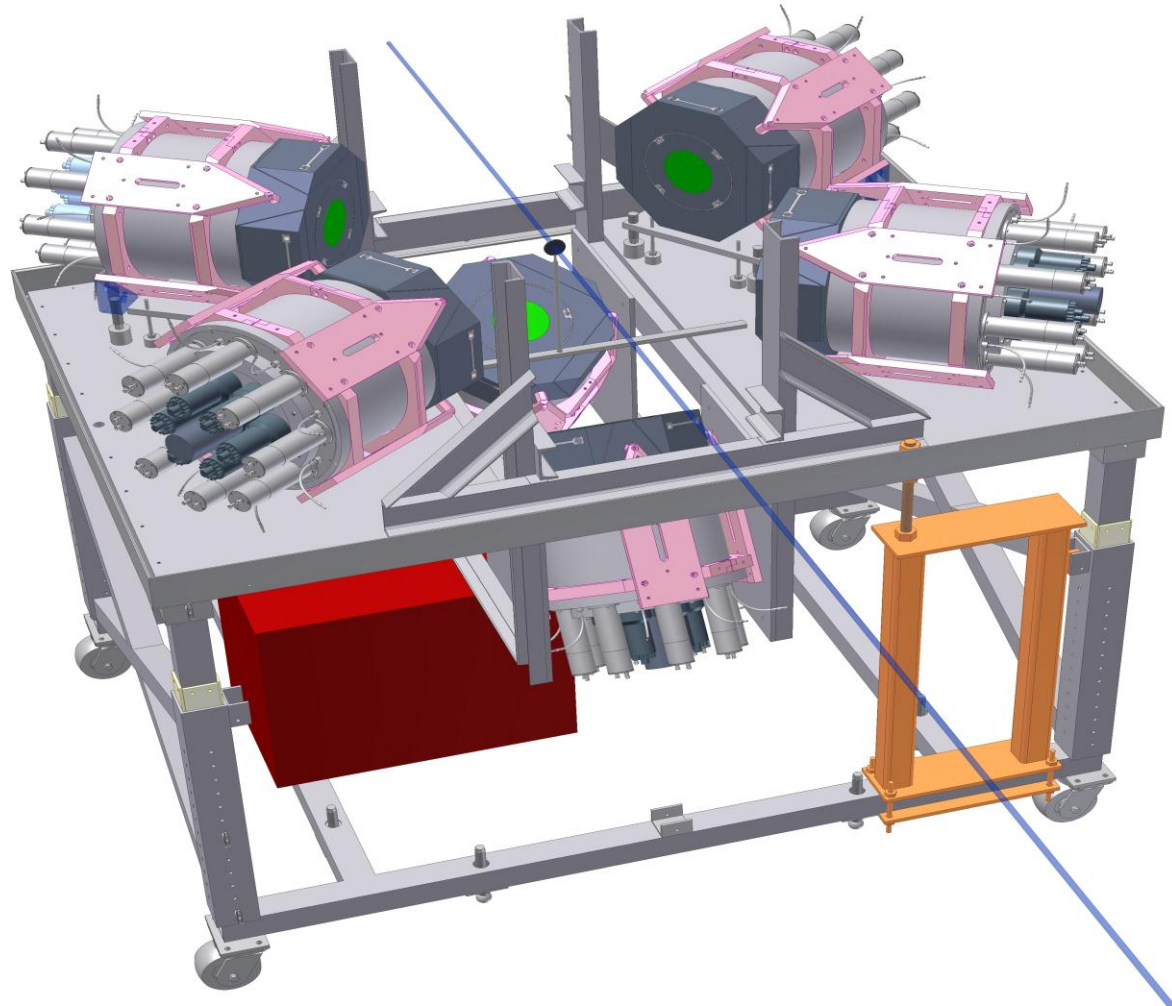
- 2" Diameter x 1/8" thick
- 9×10^{21} nuclei/cm²

6 Detectors

- 3 @ $\theta=60(55)$ (Left, Right, Down)
- 3 @ $\theta=120(125)$ (Left, Right, Down)
- $\Delta\Omega=55$ msr

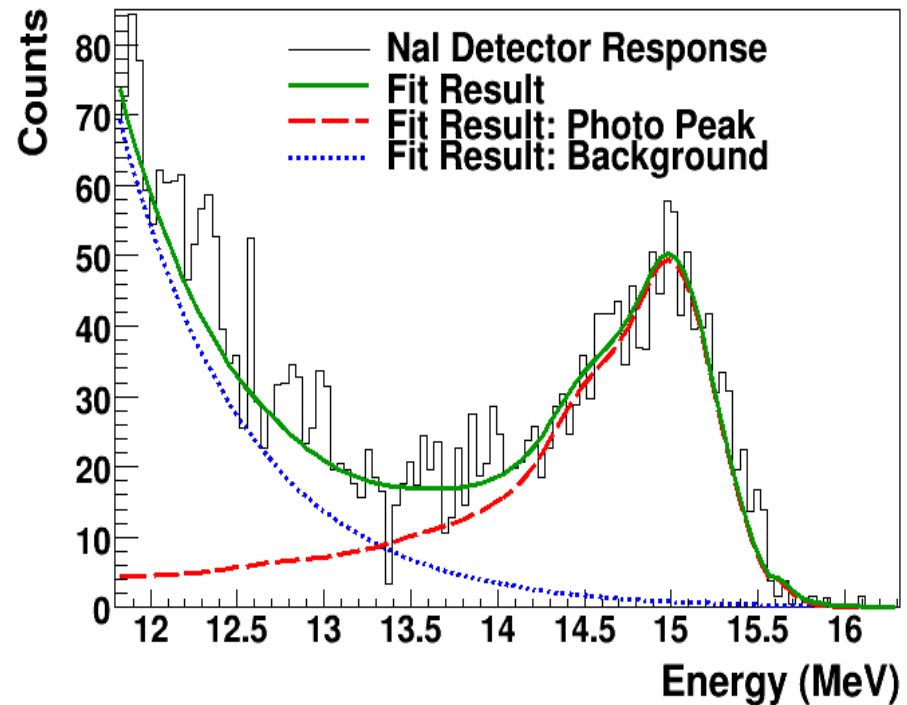
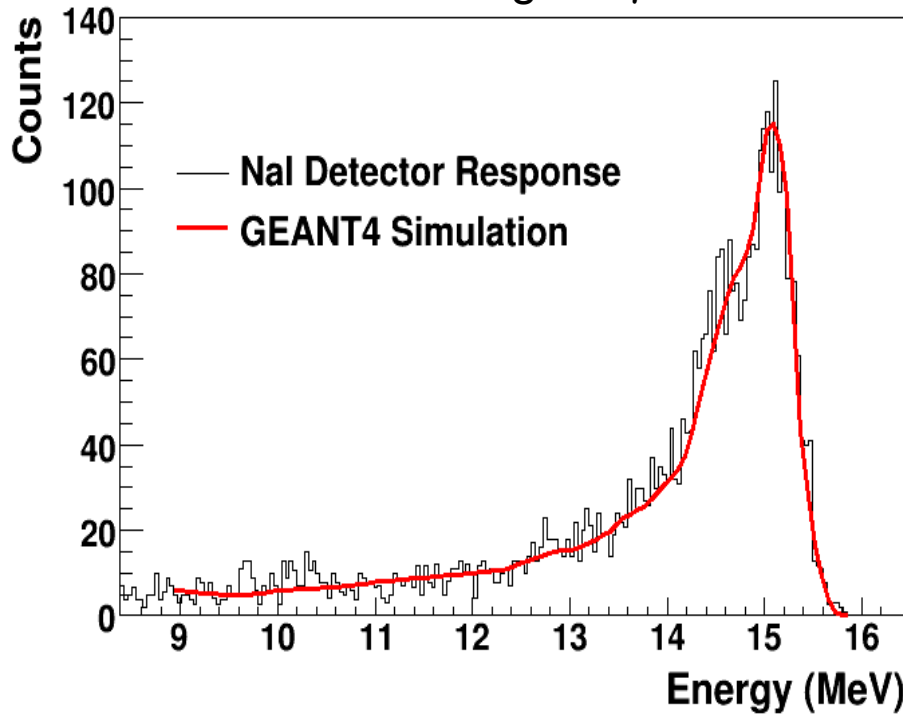
12mm collimated HI γ S beam

- 3×10^7 γ 's/sec
- $\Delta E/E=2.5$ %
- $E_\gamma = 15-26$ MeV



Analysis

Fit ^{12}C NRF spectra with GEANT4 simulation to determine Response Function for monoenergetic γ s



Fit Data with Lineshape + Background
Subtract Background

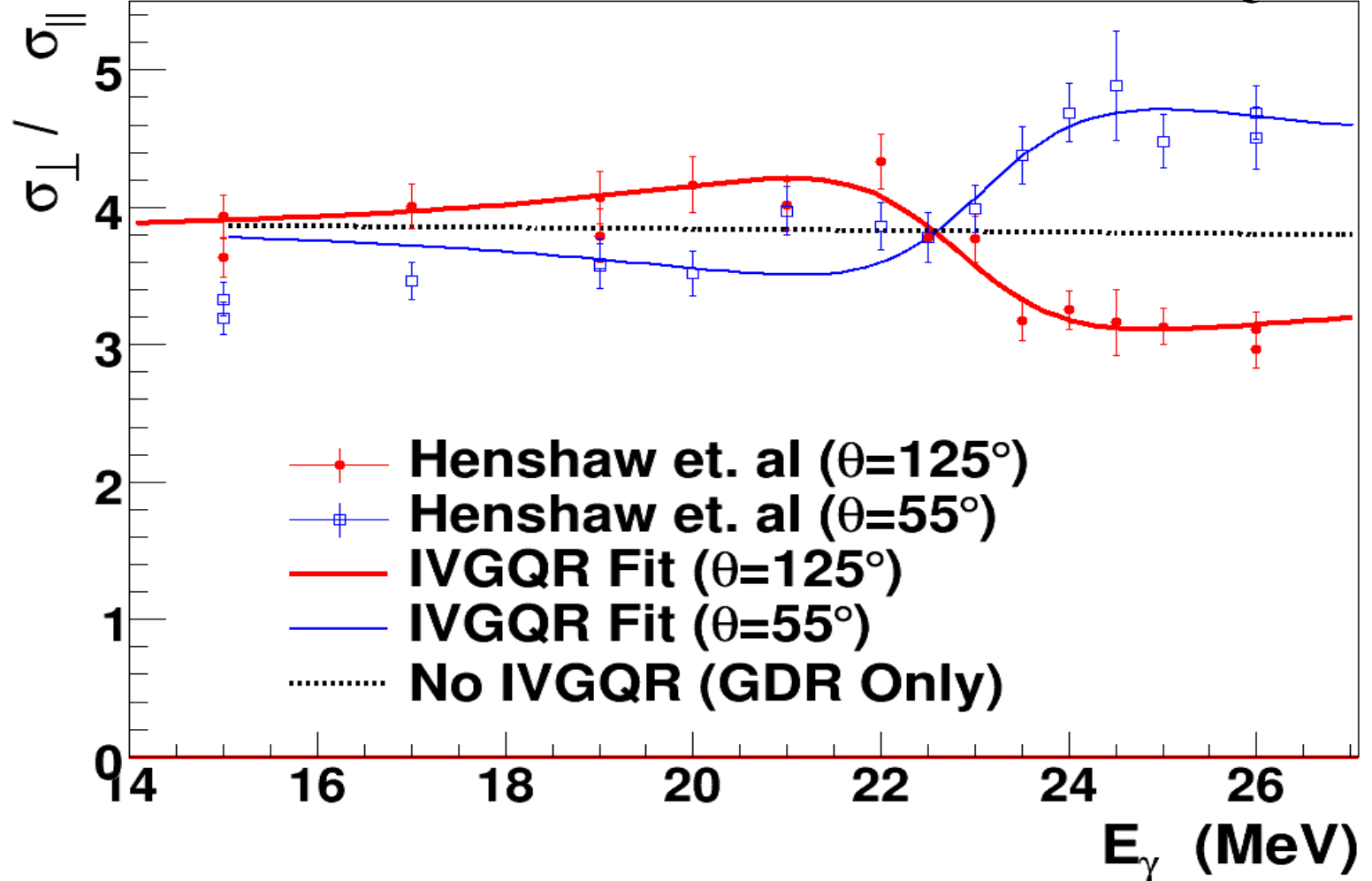
Mumbai talk 2010 Sum Resulting Data

Results

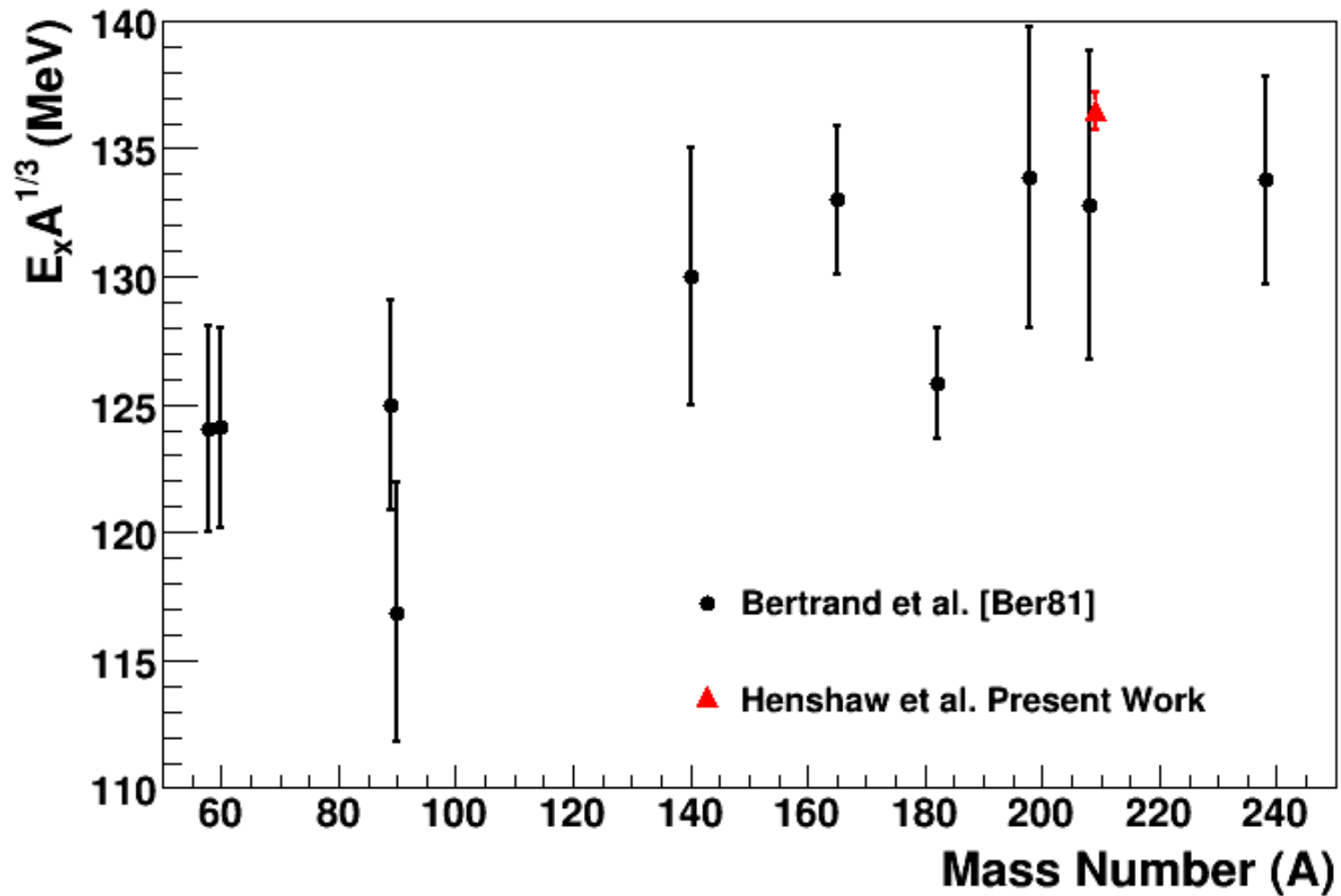
$E=23\pm 0.13$ MeV

$\Gamma=3.9 \pm 0.7$ MeV

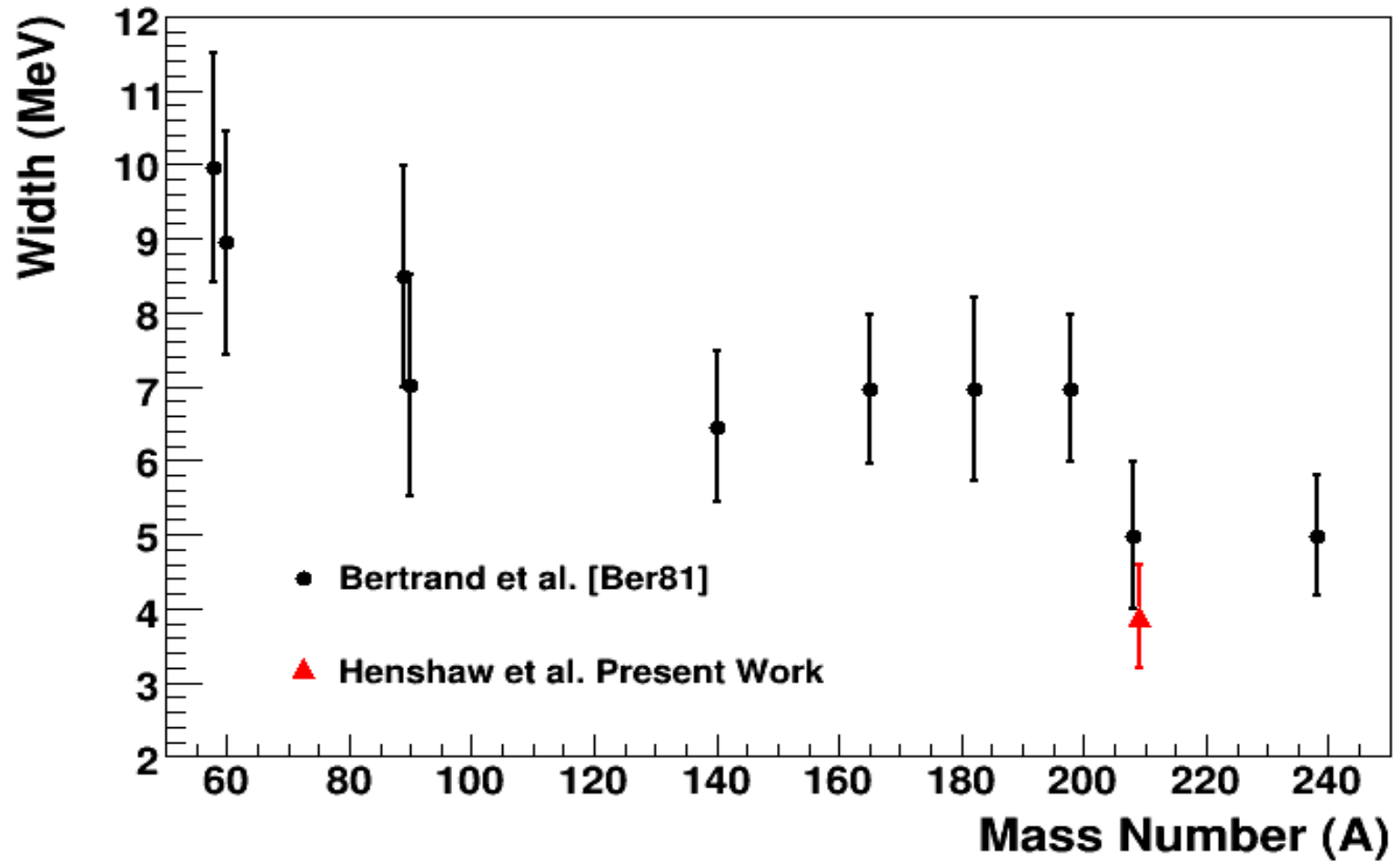
$SR=0.6 \pm 0.04$ IVQ-EWSRs



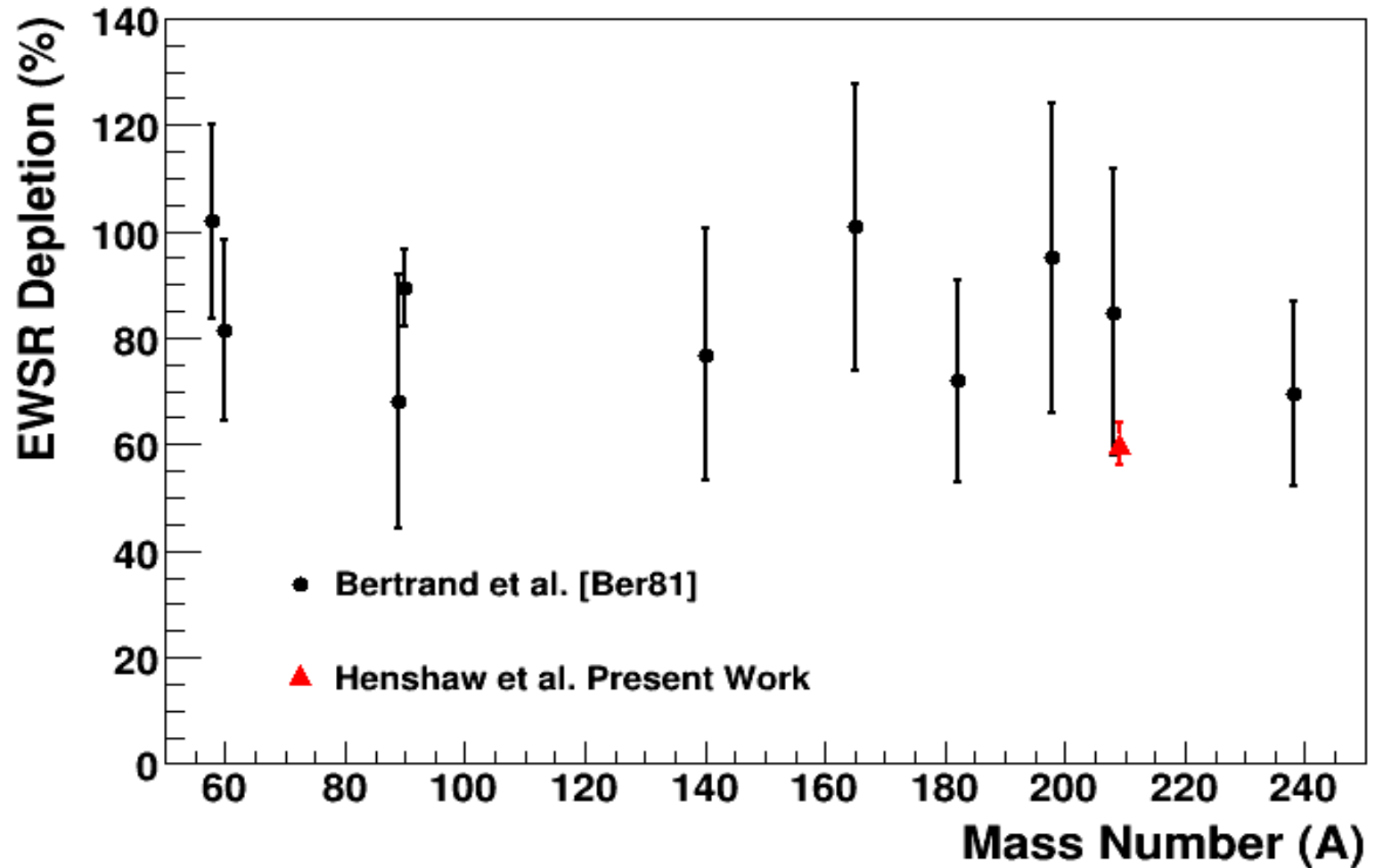
Results



Results



Results



Summary

HI γ S beams have made it possible to obtain data at a new level of precision. Results to date include:

A determination of the splittings of the p-wave amplitudes in deuteron photodisintegration.

Verification of the positive value of the GDH integrand above 10 MeV for the deuteron

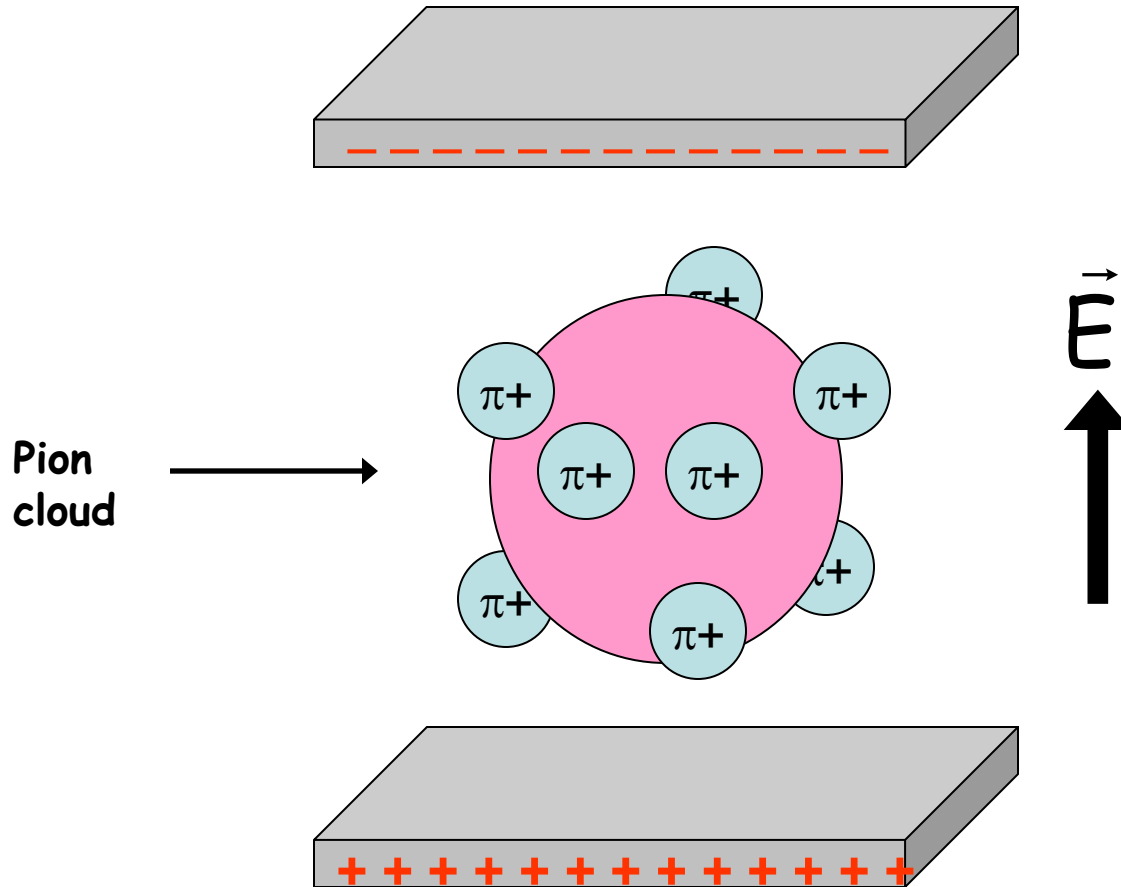
A first determination of the forward spin polarizability of the deuteron

Precise determination of the IVGQR in ^{209}Bi

The Compton @HI γ S Program

1. *Use linearly polarized γ s at ~ 100 MeV to obtain accurate values for α and β of the proton.*

Proton electric polarizability



Electric polarizability: proton between charged parallel plates

• Proton electric and magnetic polarizabilities from real Compton scattering[†]

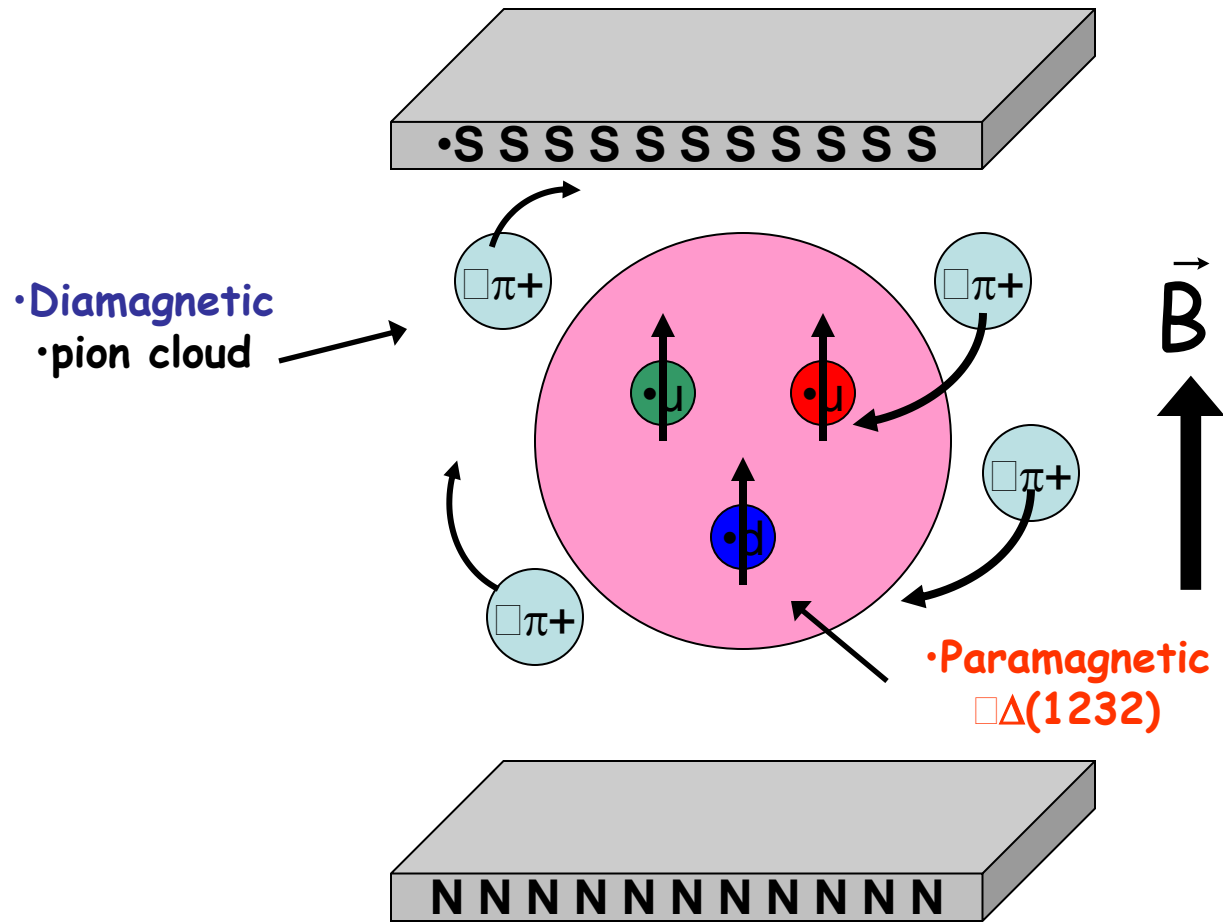
$$\alpha = (12.0 \pm 0.6) \times 10^{-4} \text{ fm}^3$$

$$\beta = (1.9 \mp 0.6) \times 10^{-4} \text{ fm}^3$$

- Some observations...
 - i. the numbers are small: the proton is very "stiff"
 - ii. the magnetic polarizability is around 20% of the electric polarizability
- Cancellation of positive paramagnetism by negative diamagnetism

•[†] M. Schumacher, Prog. Part. and Nucl. Phys. **55**, 567 (2005) and PDG.

•Proton magnetic polarizability



•Magnetic polarizability: proton between poles of a magnetic

Linearly polarized γ s allow for independent measurements of the electric (α) and the magnetic (β) polarizabilities of the proton.

(Leonard Maximon, PRC39, 347 (1989))

Present values ($\times 10^{-4} \text{ fm}^3$)

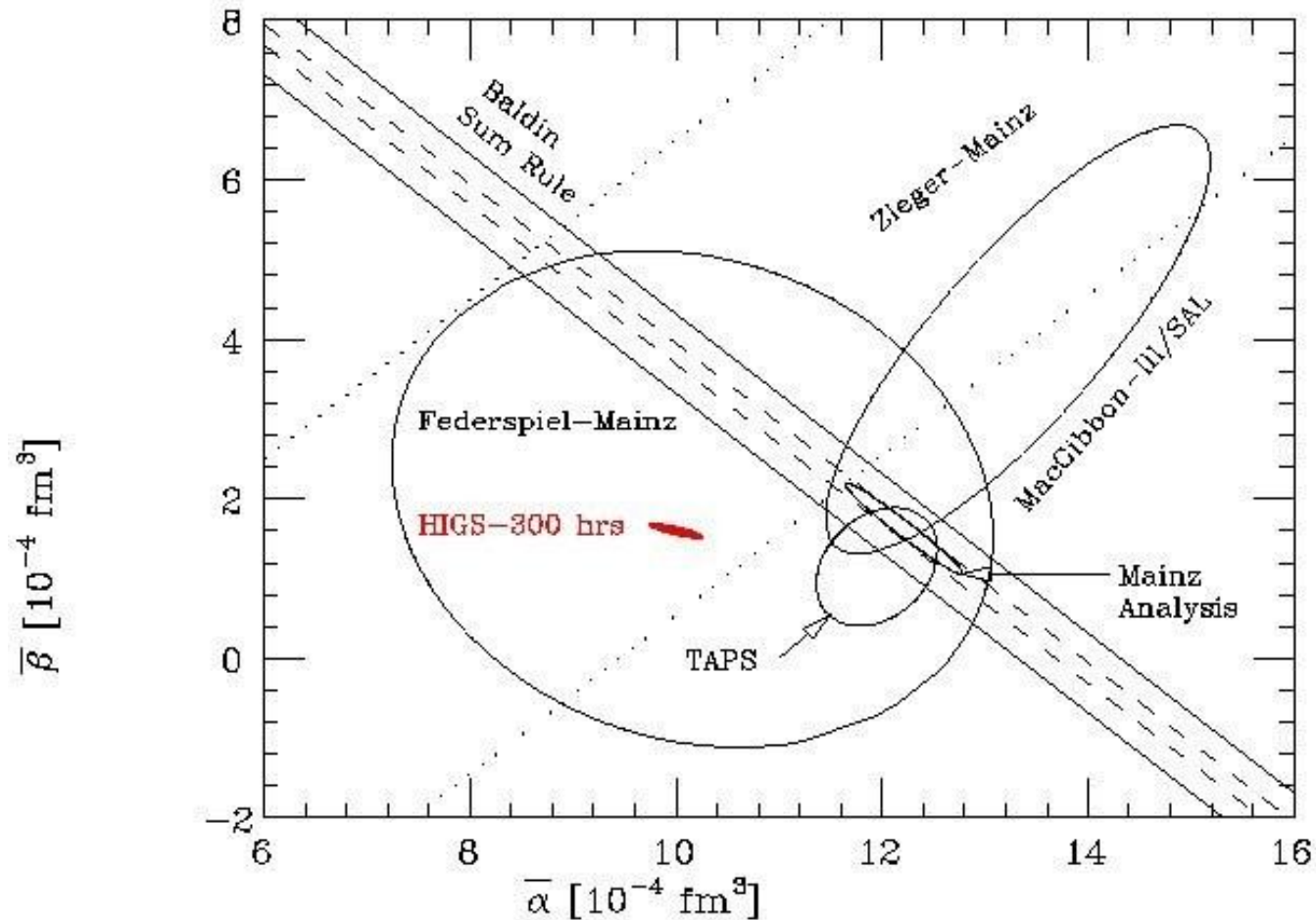
$\alpha = 12.0 \pm 1.1$ (stat + sys) ± 0.5 (th); $\beta = 1.9 \pm 0.8$ (stat + sys) ± 0.5 (th)

$$\left. \frac{d\sigma_{\perp}}{d\Omega} \right|_{\theta=90} - \left. \frac{d\sigma_{\perp}^{pt}}{d\Omega} \right|_{\theta=90} = -K\alpha$$

$$\cos^2\theta \left(\frac{d\sigma_{\perp}}{d\Omega} - \frac{d\sigma_{\perp}^{pt}}{d\Omega} \right) - \left(\frac{d\sigma_{\parallel}}{d\Omega} - \frac{d\sigma_{\parallel}^{pt}}{d\Omega} \right) = K\beta \cos\theta \sin^2\theta$$

where $K = 2 \left(\frac{e^2}{Mc^2} \right) \left(\frac{\omega'}{\omega} \right)^2 \omega \omega'$

- Determination of the electric and magnetic polarizabilities of the proton using 100% linearly polarized gammas @ HIγS – a ~300 hr experiment with a beam intensity of $5 \times 10^7 \gamma/s$ **will yield 5% errors on α**
□ (now ~15%) and β (now ~40%).



Compton scattering from the deuteron— determining the neutron polarizabilities

- This determines the *isoscalar polarizabilities* α_N and β_N , which lead to the neutron polarizabilities using the known values of the proton.
- *Data to date:*
- **Illinois**, $E_\gamma = 49, 69 \text{ MeV}$ M. Lucas, PhD thesis, 1994
- **Saskatoon**, $E_\gamma = 95 \text{ MeV}$ D. L. Hornidge et al. PRL 84, 2334(2000)
- **Lund**, $E_\gamma = 60 \text{ MeV}$ M. Lundinet et al, PRL 90 (2003) 192501

•A global fit to all existing γd data using the Baldin sum rule. The results are

$$\alpha_E^s = (11.3 \pm 0.7 \text{ (stat)} \pm 0.6 \text{ (Baldin)}) \times 10^{-4} \text{ fm}^3$$

$$\beta_M^s = (3.2 \pm 0.7 \text{ (stat)} \pm 0.6 \text{ (Baldin)}) \times 10^{-4} \text{ fm}^3$$

which indicates, by comparing to the proton values, that *the n and p polarizabilities are essentially the same within experimental errors.*

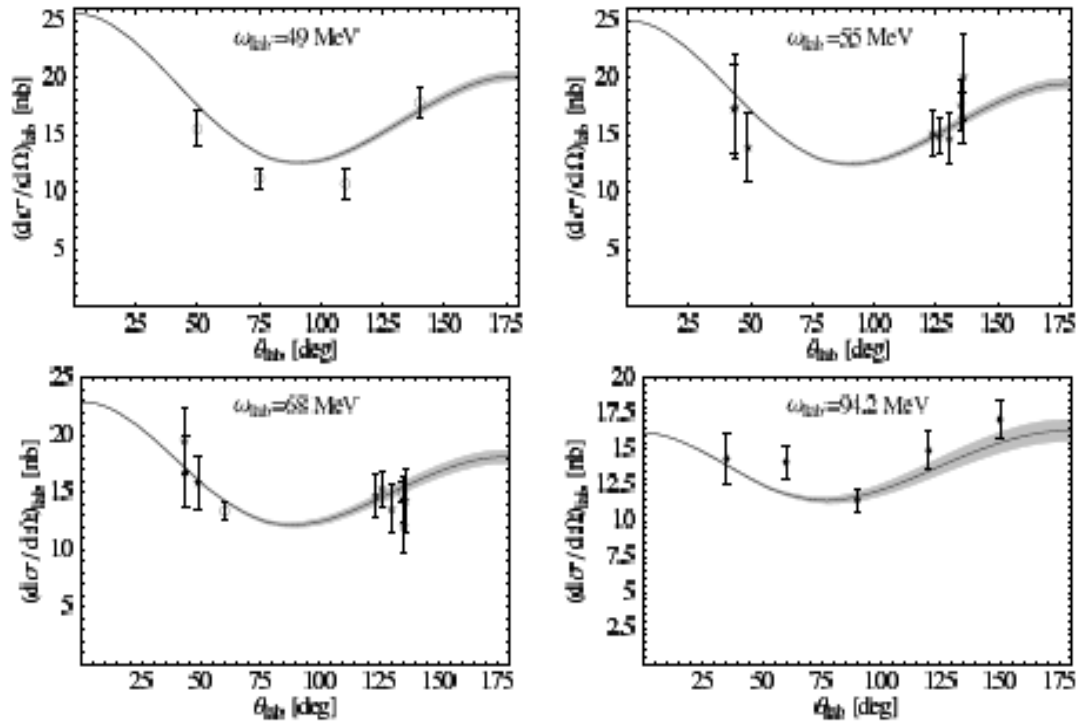


Figure 18: Results from a global fit of α_E^s to all existing elastic γd data, using the chiral wave function [36]. β_M^s is fixed via the Baldin sum rule, Eq. (4.3). The grey bands are derived from our statistical errors.

Compton on the deuteron @ HI γ S

- The *HINDA spectrometer* and a liquid *scintillating target* will be used in these experiments.
- Angular distributions will be measured in 10 MeV steps between 30 and 80 MeV. **We expect to obtain 1.5% statistics in each of 8 detectors at 6 energies in ~300 hours.** The absolute cross section will be determined to an accuracy of ~3%.
- These measurements will *determine the neutron polarizabilities to an accuracy of ~20%.*

Spin polarizabilities.

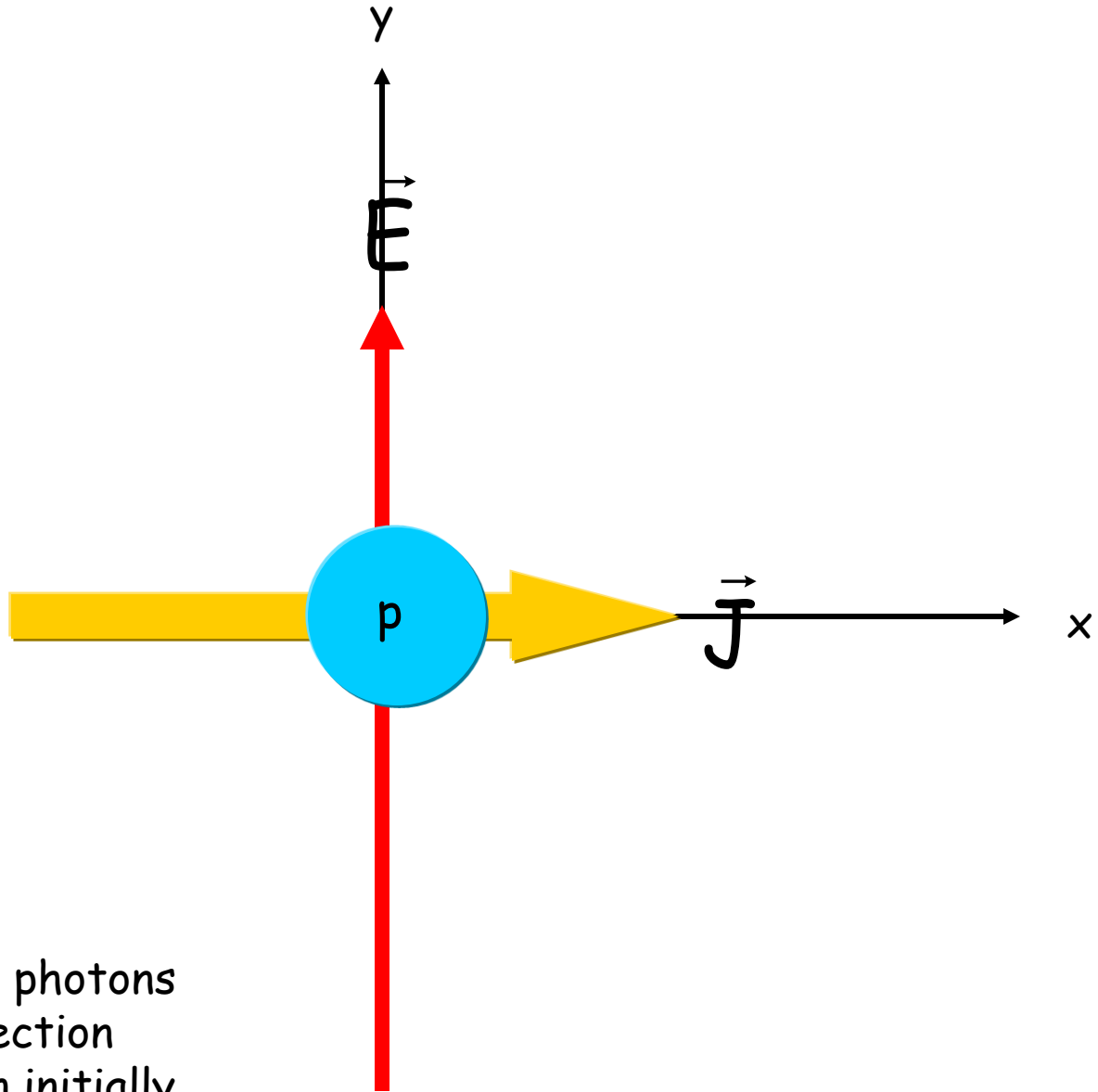
- They tell us about the response of the spin of the nucleon to the polarization of the photons. The stiffness of the spin can be thought of as arising from the nucleon's spin interacting with the pion cloud.
- Measuring these requires circularly polarized beams and polarized targets – ideally suited to HI γ S.
- Polarized protons will be provided by our frozen-spin target. A polarized ^3He target will be used to obtain the neutron spin-polarizabilities.

• The spin-polarizabilities of the nucleon

- At $O(\omega^3)$ four new nucleon structure terms that involve nucleon spin-flip operators enter the RCS expansion.

$$H_{eff}^{(3),spin} = -\frac{1}{2}4\pi \left(\gamma_{E1E1} \vec{\sigma} \cdot \vec{E} \times \dot{\vec{E}} + \gamma_{M1M1} \vec{\sigma} \cdot \vec{B} \times \dot{\vec{B}} - 2\gamma_{M1E2} E_{ij} \sigma_j H_j + 2\gamma_{E1M2} H_{ij} \sigma_j E_j \right)$$

- A rotating electric field will induce a precession of the proton spin around the direction of the polarized photon, with a rate proportional to the spin-polarizability.

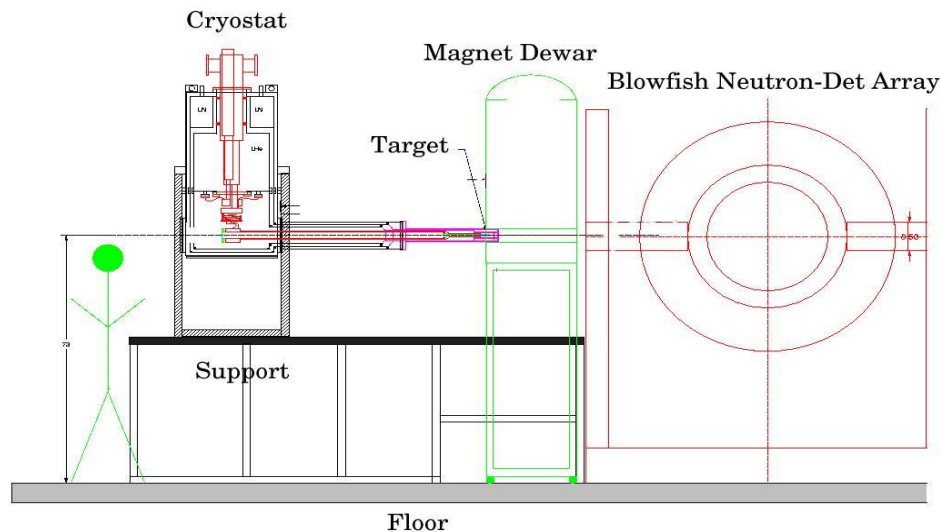


Circularly polarized photons
moving in the z-direction
incident on a proton initially
polarized in the x-direction

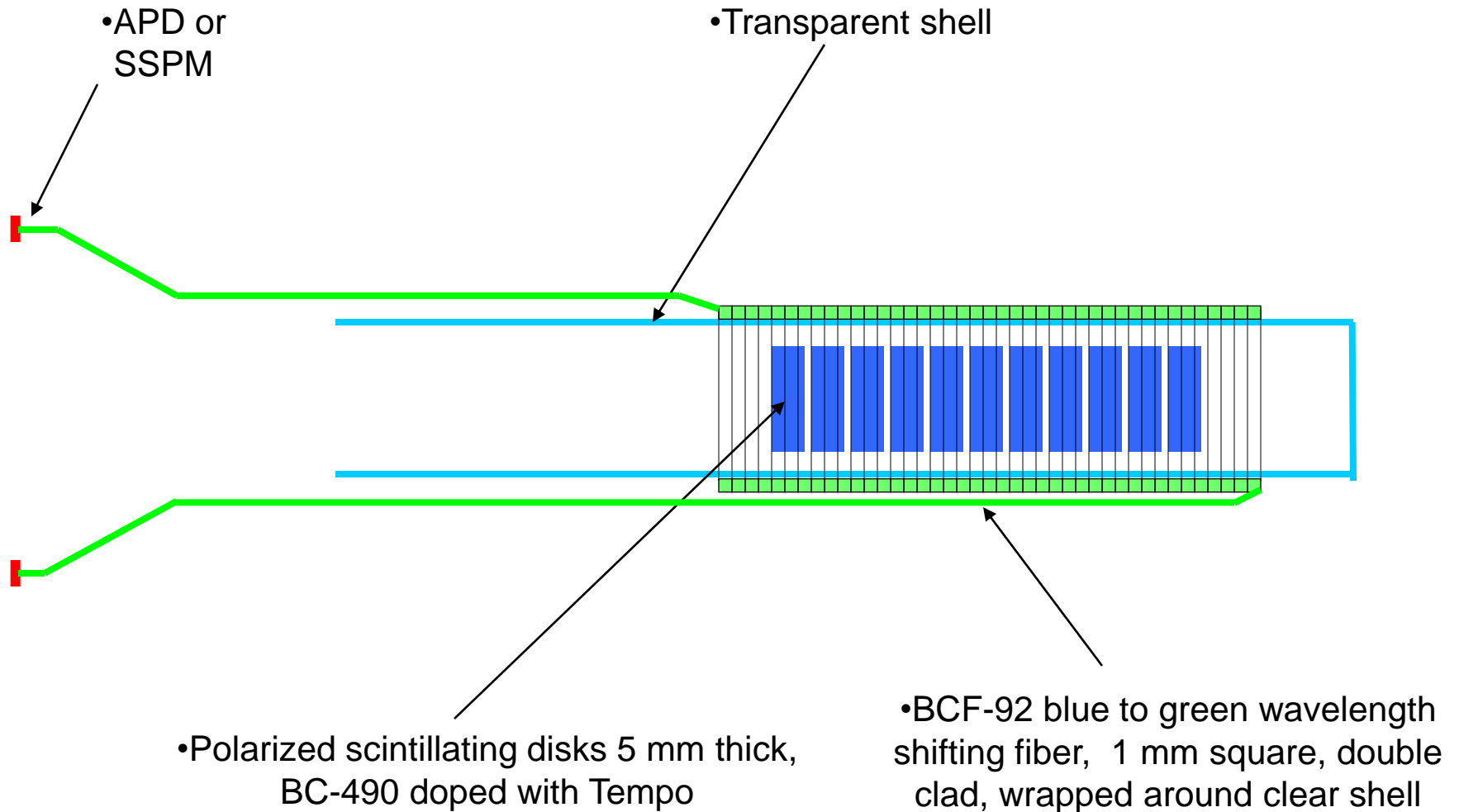
- ***Proton spin-polarizabilities will be measured using a scintillating frozen-spin polarized target***
 - **Rory Miskimen et al., U. Mass.**
- Simulations have been performed. A working prototype is under construction.
 - *The initial experiment will run near 100 MeV.*

□ ^3He Frozen Spin Polarized Target (HIFROST)

- • Butanol
- • Polarization $\sim 80\%$
- • Polarizing Field $\sim 2.5\text{ T}$
- • Holding Field $\sim 0.6\text{ T}$



•Light capture with wavelength shifting fibers

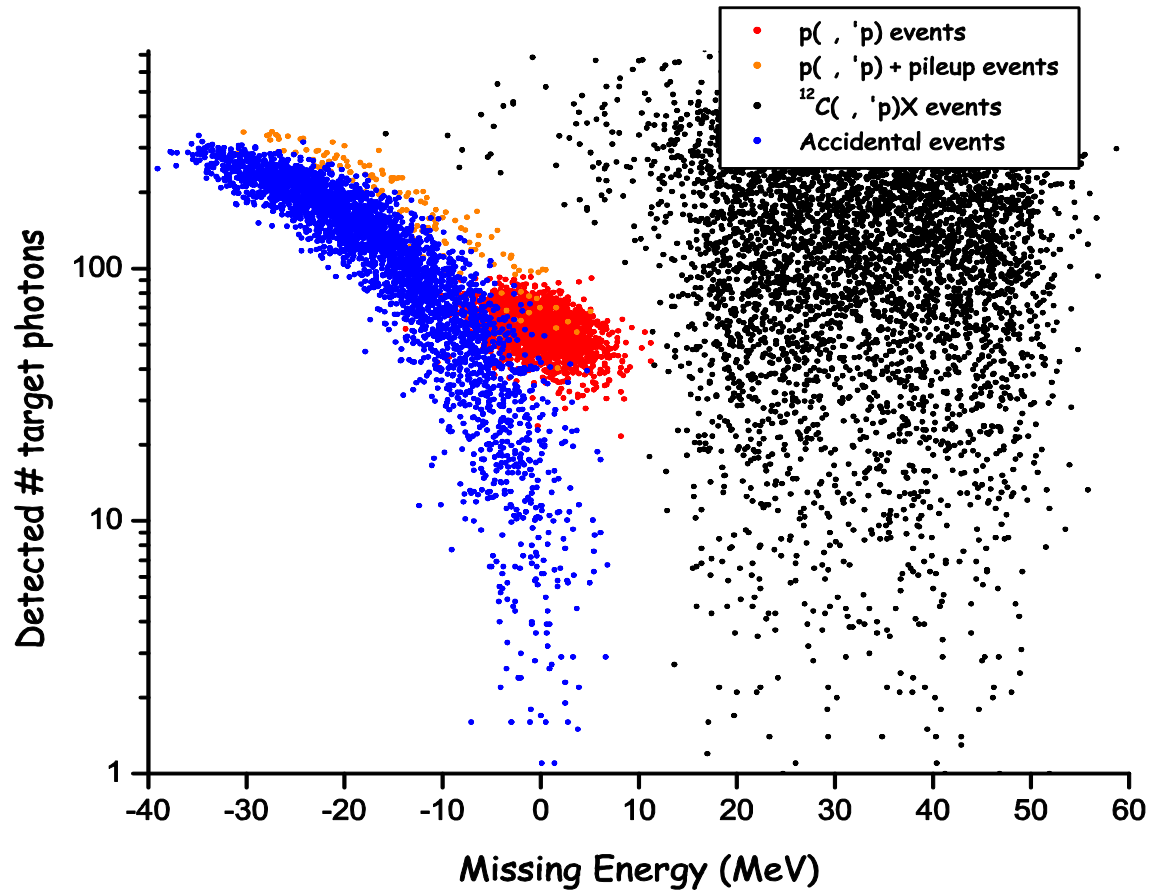


•Overall light transport efficiency \approx 2%

Mumbai talk 2010

Results of a simulation using the scintillating Butanol target and a HINDA detector (performed by Rory Miskimen).

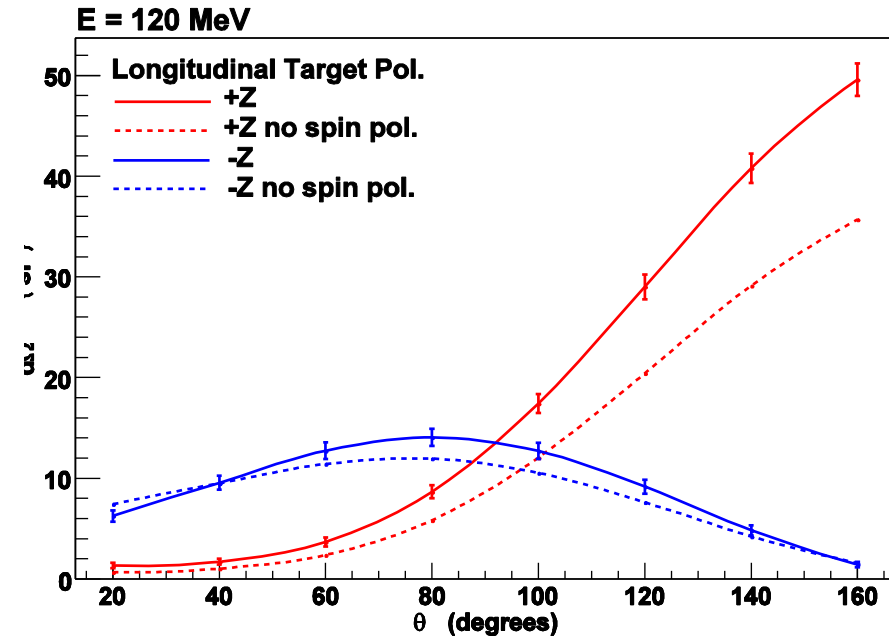
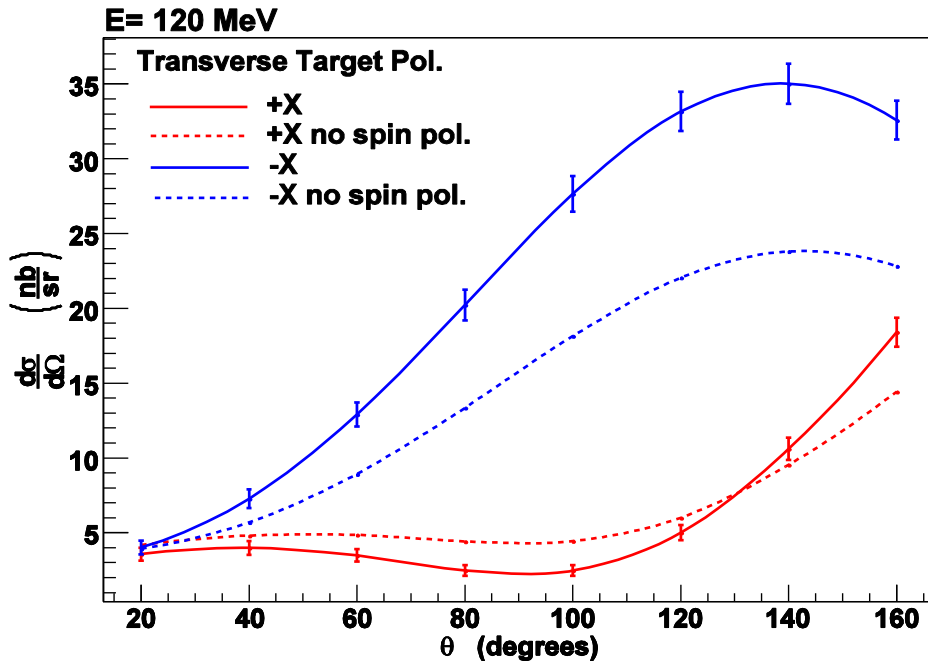
(Missing Energy = $E_{beam} - E_{NaI} - E_{target}$)



Count rate calculations and projections

- Used the theoretical study of Hildebrandt et al. (Eur. Phys. J. A20 (2004) 329 which examined the sensitivity of Compton scattering to the spin-polarizabilities.
- Target thickness: 2.6×10^{23} p/cm² ; 80% polarization
- Beam intensity: 1×10^7 γ /s @ 120 MeV
- The HINDA array with dets. 75 cm from the target
- Running time: 200 hrs. longitudinal, 200 hrs. transverse
- Spin pols. were fit to *pseudo-data* using theoretical model of Hildebrandt to generate the uncertainties.

Running at 120 MeV with both transverse and longitudinal targets will produce ~5% results for the dipole spin polarizabilities in ~400 hours of beam time (200 hrs. transverse polarization and 200 hrs. longitudinal).



- *Total beam time for proton measurement: 400 hrs*

- *100 hrs for each target spin orientation*

• Theory curves: Hildebrandt, Griesshammer, Hemmert,

• Nucl-th/0308054

Mumbai talk 2010

- Projected HI γ S measurements on Nucleon Spin
- Polarizabilities (all x 10⁻⁴ fm⁴)—Theoretical values
- are from Gellas, Hemmert and Meissner PRL 85 (2000)14.

•Proton HI γ S projected uncertainties	•Neutron HI γ S projected uncertainties
• $\gamma^p_1=1.1 \pm 0.10$	• $\gamma^n_1=3.7 \pm 0.43$
$\gamma^p_2=-1.5 \pm 0.36$	$\gamma^n_2=-0.1 \pm 0.03$
• $\gamma^p_3=0.2 \pm 0.24$	• $\gamma^n_3=0.4$
• $\gamma^p_4=3.3 \pm 0.17$	• $\gamma^n_4=2.3 \pm 0.57$

Conclusion:

- Measuring the spin-polarizabilities of the nucleon is an important next step. These are fundamental structure constants of the nucleons. The beam, targets, and detectors are now available for these experiments.
- Can measure the polarizabilities at HIGS with a precision of from 0.2 to $0.4 \times 10^{-4} \text{ fm}^4$, which is sufficient to test and differentiate between theoretical models. Full Lattice QCD calculations are imminent.

Summary

In the near future we anticipate--

A direct measurement of the GDH integrand and γ_0 of the deuteron below pion threshold

Precise determination of electric and magnetic polarizabilities of the proton and the neutron

First determination of the spin polarizabilities of the nucleons.

And more!

A New Method for Identifying Special Nuclear Materials Based Upon Polarized

A TUNL/HI γ S Project funded by the NSF/DNDO through their Academic Research Initiative program

H. R. Weller—PI

M. Ahmed and Y. Wu -- Co PIs

Collaborators:

N. Brown, S.S. Henshaw, H. J. Karwowski, J. M. Mueller, S. Stave, B. A. Perdue, J. R. Tompkins—TUNL

B. Davis and D. Markoff—NCCU

G. Feldman—GWU

L. Myers—UIUC

M. S. Johnson--LLNL

Introduction

- **Premise: Linearly polarized γ rays** having energies between threshold and 20 MeV can be a useful tool for the interrogation of materials
- Induce the emission of **several MeV neutrons** which can then be detected as a function of energy and emission angle relative to the plane of polarization
- In fissionable nuclei, **energetic neutrons** are produced even at energies effectively below (γ, n) threshold

—

Formalism

- For **unpolarized** γ -ray beams, the angular distribution of the outgoing neutrons assuming pure electric dipole absorption can be written as:

$$\sigma(\theta) = A_0(1 + a_2 P_2(\cos \theta))$$

where $a_2 = A_2/A_0$, P_2 is the second Legendre polynomial

Using Satchler's expressions for **linearly polarized** γ -rays (Proc. Phys. Soc., 68A:1041, 1955), when both detectors are at 90 degrees:

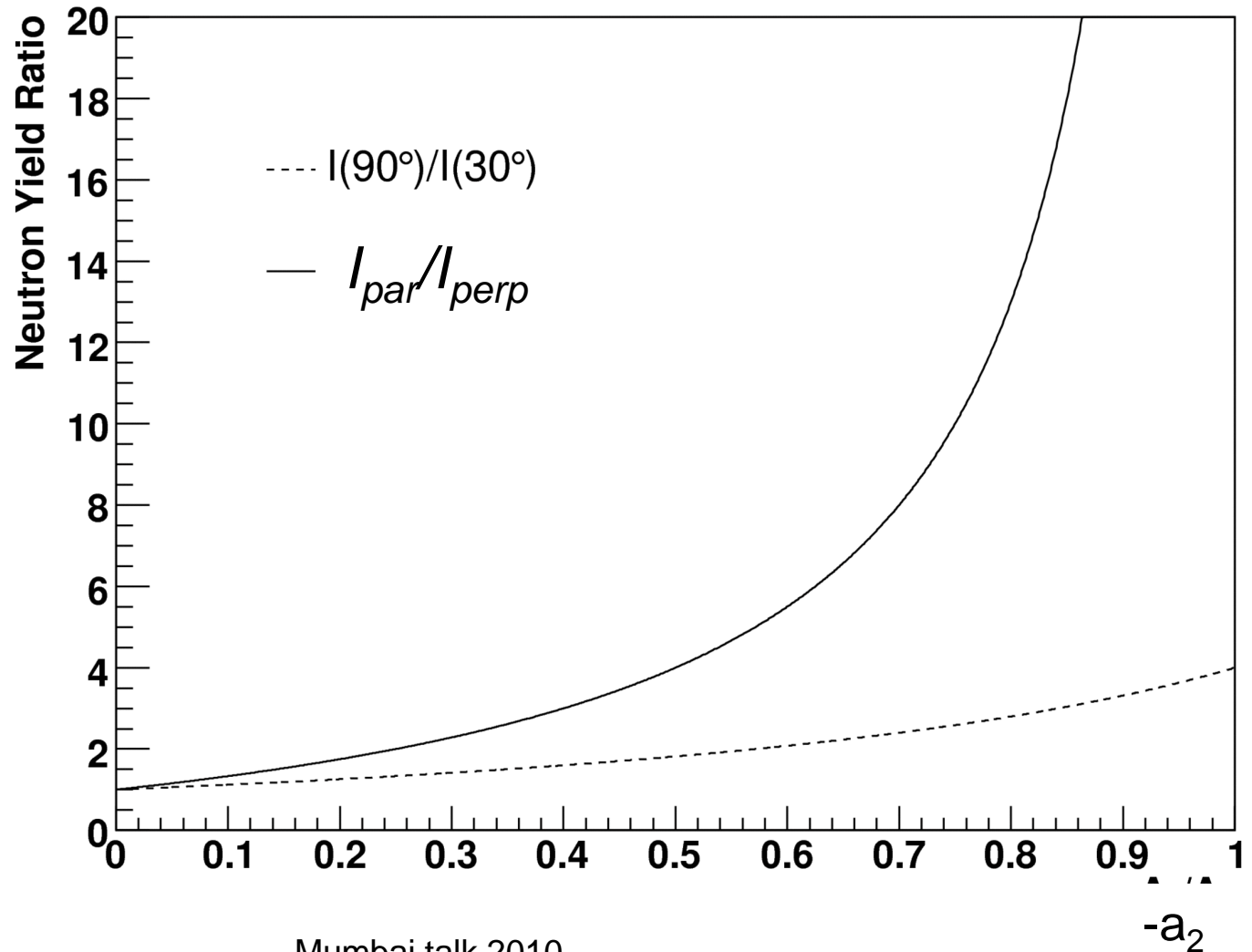
$$I_{par} = A_0(1 - 2a_2)$$

$$I_{perp} = A_0(1 + a_2)$$

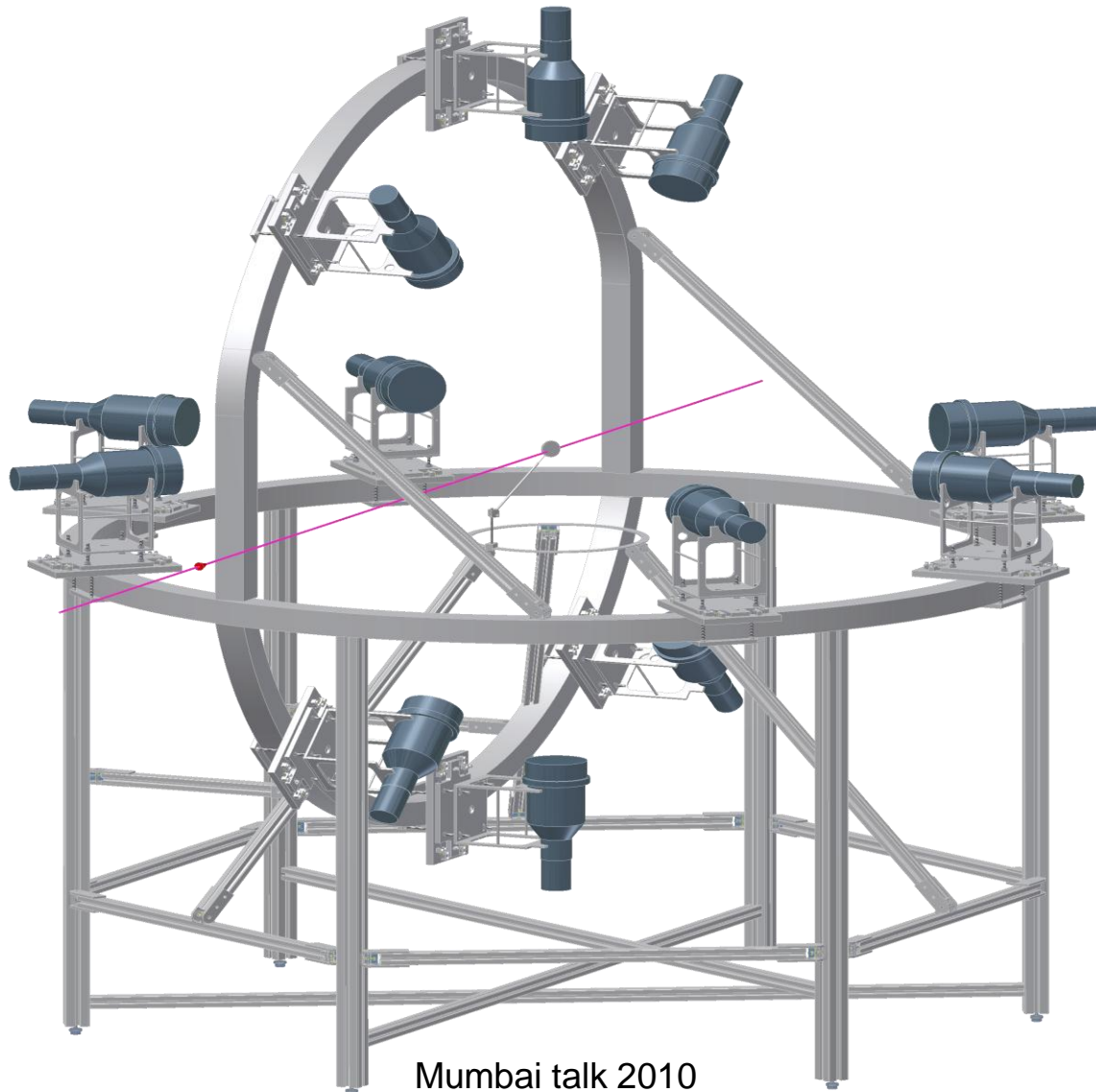
I_{par}/I_{perp} depends only on a_2

Sensitivity when using 2-detectors

- Linearly polarized beam
increases sensitivity over unpolarized measurement

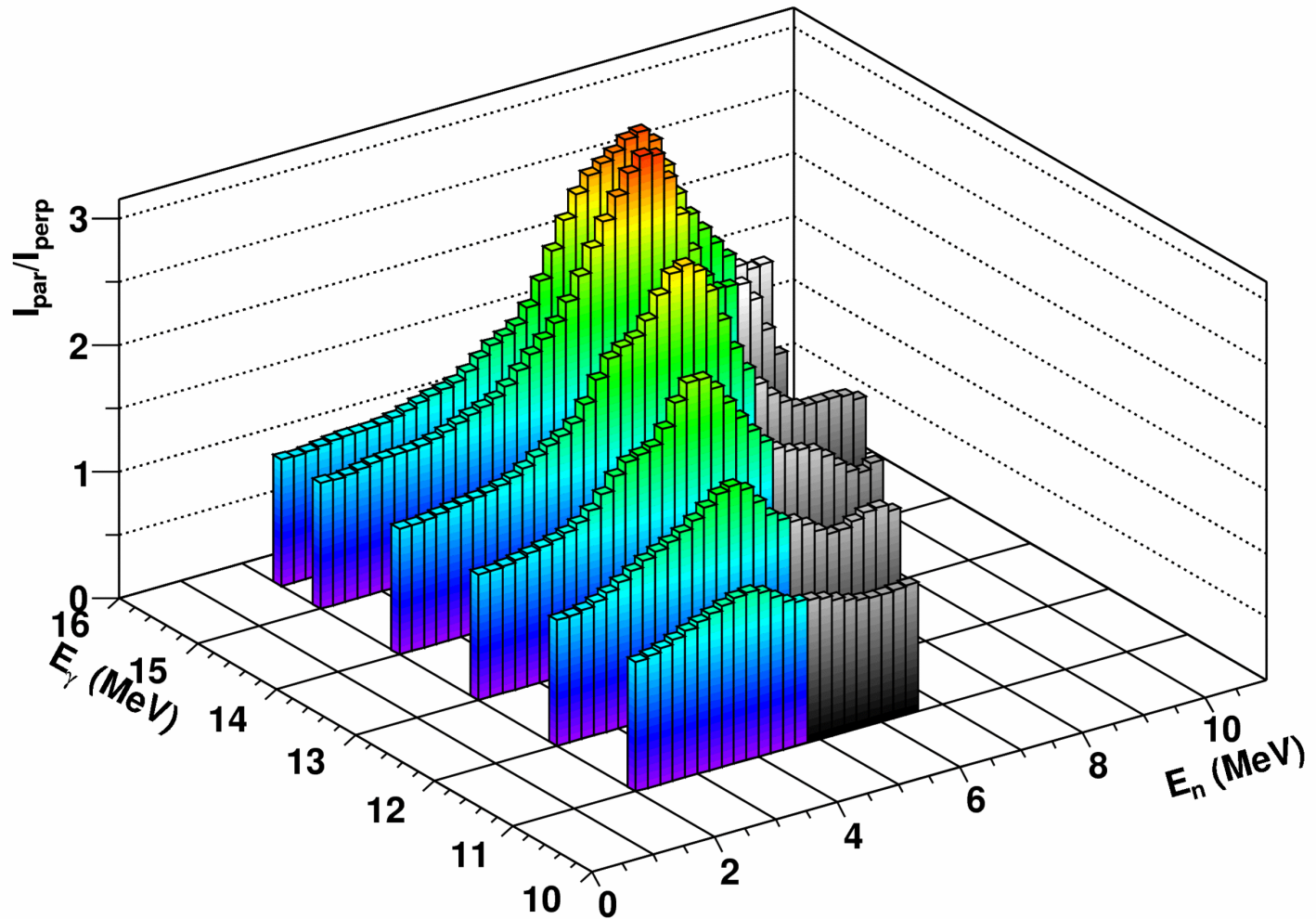


Flight path is one meter. Up, down, left and right detectors at 55, 90 and 125 degrees.



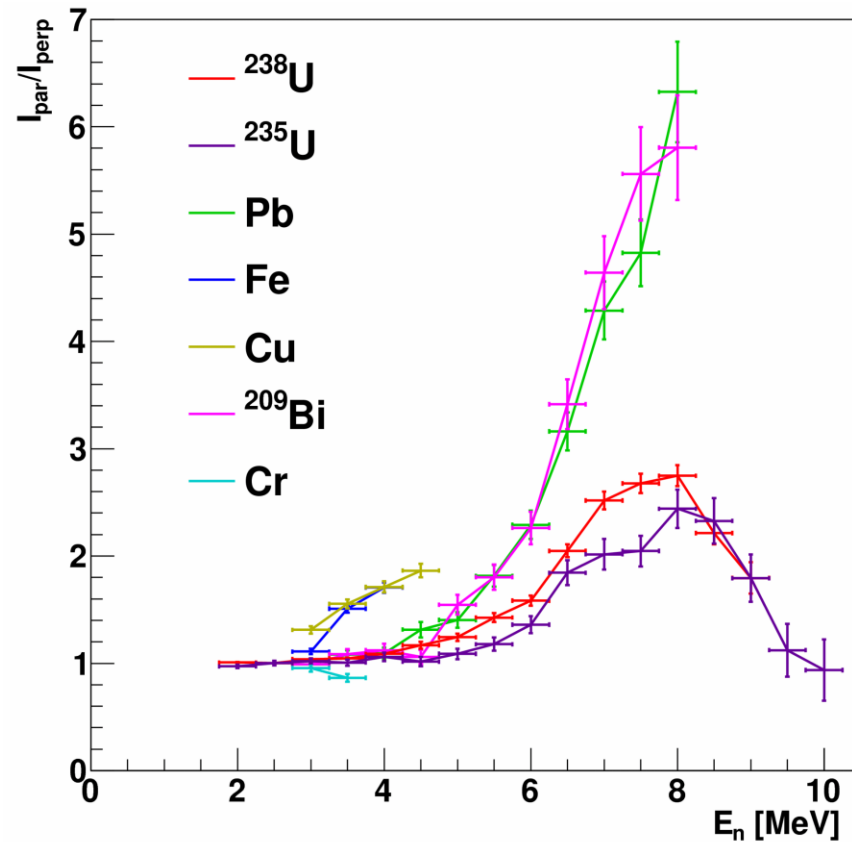
Mumbai talk 2010

Preliminary results from the Feb. 22-28, 2010 run for ^{238}U



Mumbai talk 2010

New data were obtained on Pb, ^{235}U , and ^{238}U ; results at 15.5 MeV are shown here and compared to results on other targets at 90°.



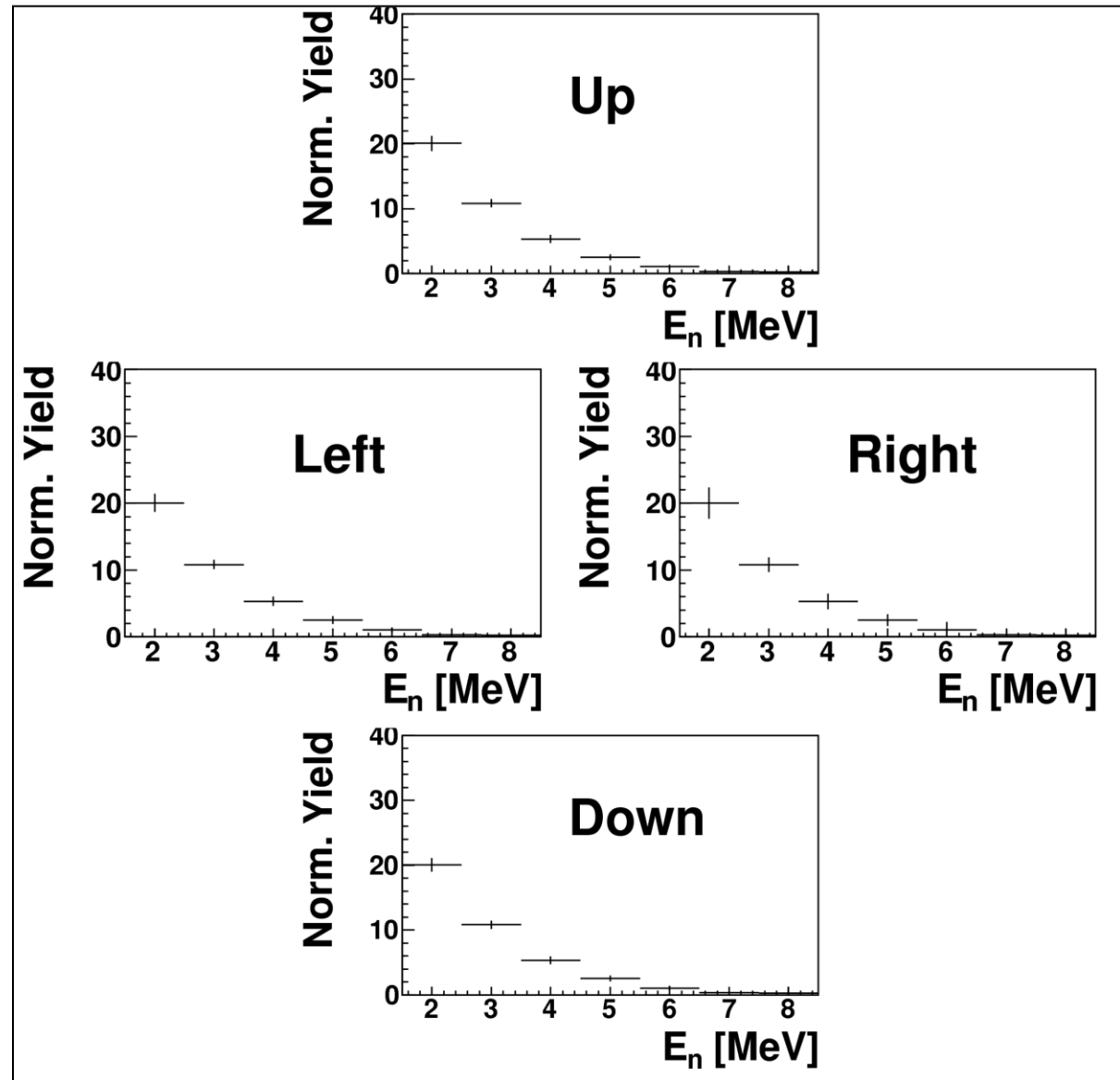
Neutron production below (γ,n) threshold

Running at a γ -ray energy of ~ 6.0 MeV and looking at neutrons above 2 MeV only produces counts for fissionable nuclei, except for d, Li and ^9Be . These can be identified by their unique spectra.

This provides a ***very promising tool*** for interrogation and is receiving further study.

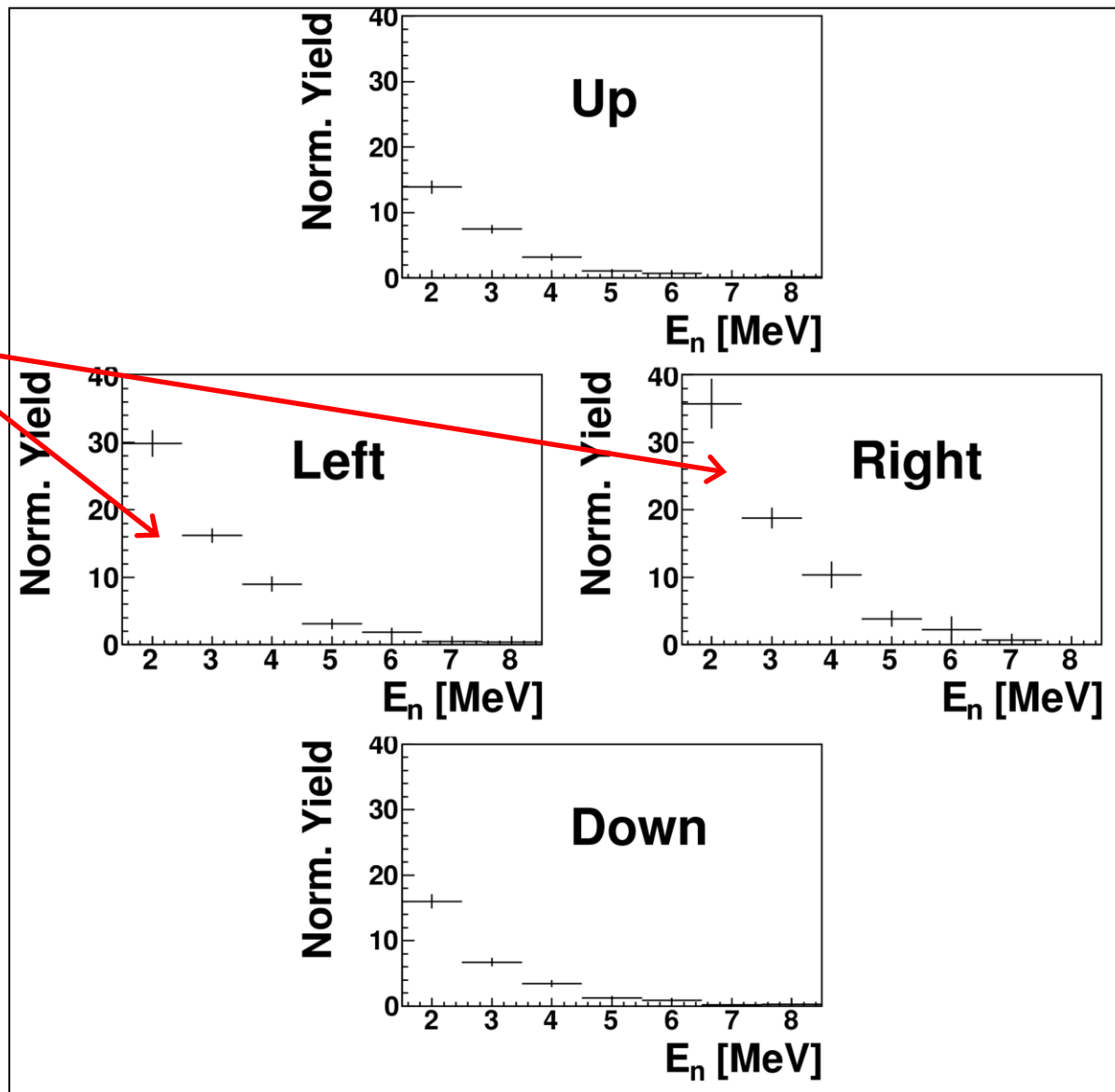
^{238}U target: 6.2 MeV Circular pol.

Same
neutron
yields both
in- and out-
of-plane, as
expected



^{238}U target: 6.2 MeV Linear Pol.

Neutron yield enhancement is observed in both in-plane detectors



Understanding the Ratio for ^{238}U

- First take the measured angular distribution of fission fragments as a function of E_γ for ^{238}U from Rabotnov [Yad. Fiz. 11, 508 (1970)]
- Using the formalism for linearly polarized γ rays from Ratzek [Z. Phys. A 308, 63 (1982)] the angular distribution of fission fragments can be written as:

$$W(\theta, \phi) = a + b\sin^2\theta + c\sin^2 2\theta + P_\gamma \cos 2\phi (d\sin^2\theta - 4c\sin^4\theta)$$

- where θ is the CM polar angle and ϕ is the CM azimuthal angle of the emitted fragment measured with respect to the plane of polarization; P_γ is the linear polarization of the γ -ray beam

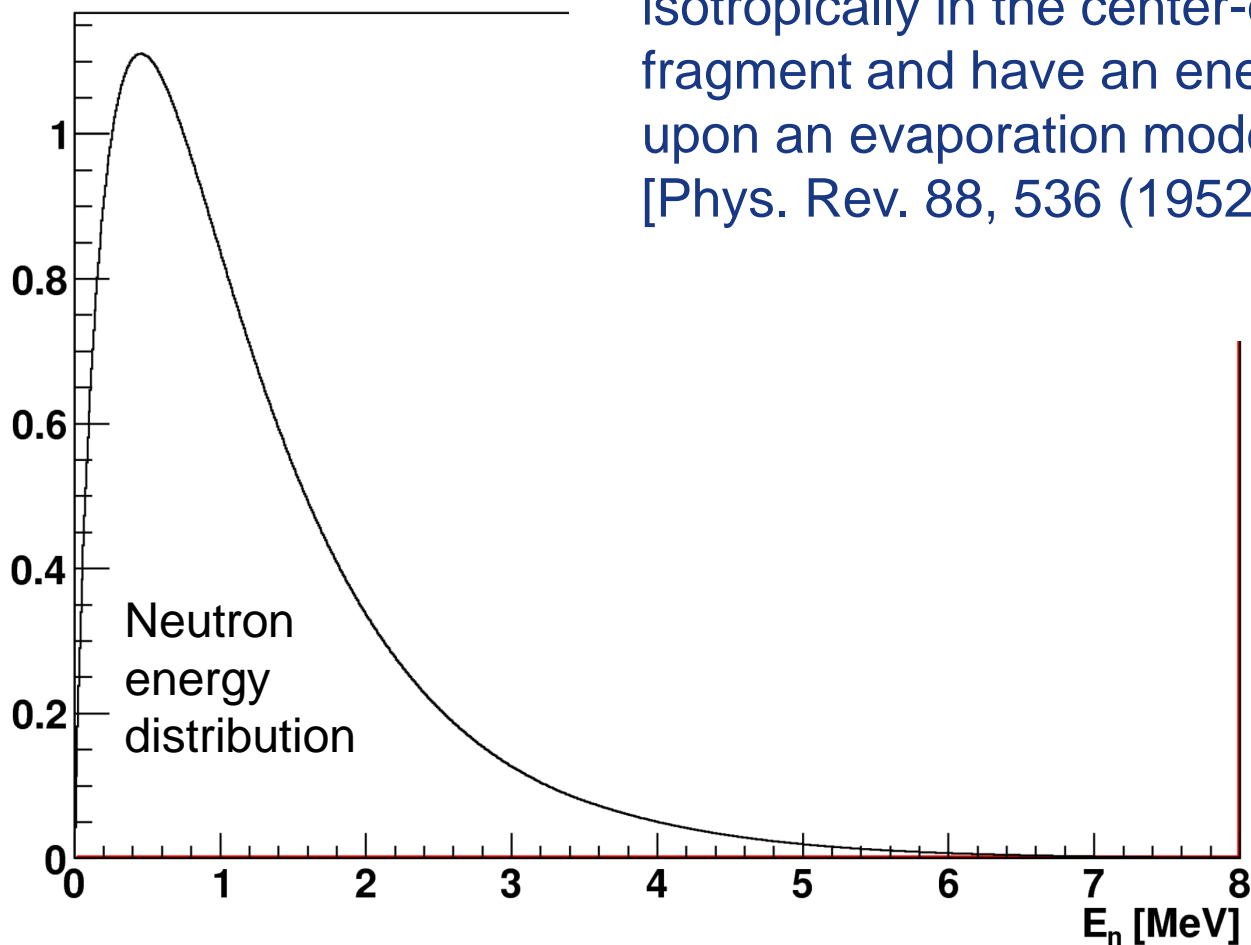
Angular Distribution of Fragments

E_γ (MeV)	a	b	c	d
5.65	0.034	0.966	0.040	1.380
5.95	0.078	0.922	0.039	1.079
6.40	0.127	0.873	0.034	1.032

- a, b, and c terms from Rabotnov
- d term can be calculated using formalism given in Ratzek with the simplification that the low lying transition states can be represented by dipole plus the $K=0$ quadrupole terms [Huizenga and Vandenbosch, *Nuclear Fission* (1973)]
- Dominated by dipole transition but with a small quadrupole contribution

Neutron energy distribution

- Then assume the neutrons are emitted isotropically in the center-of-mass frame of each fragment and have an energy distribution based upon an evaporation model from Fraser [Phys. Rev. 88, 536 (1952)]



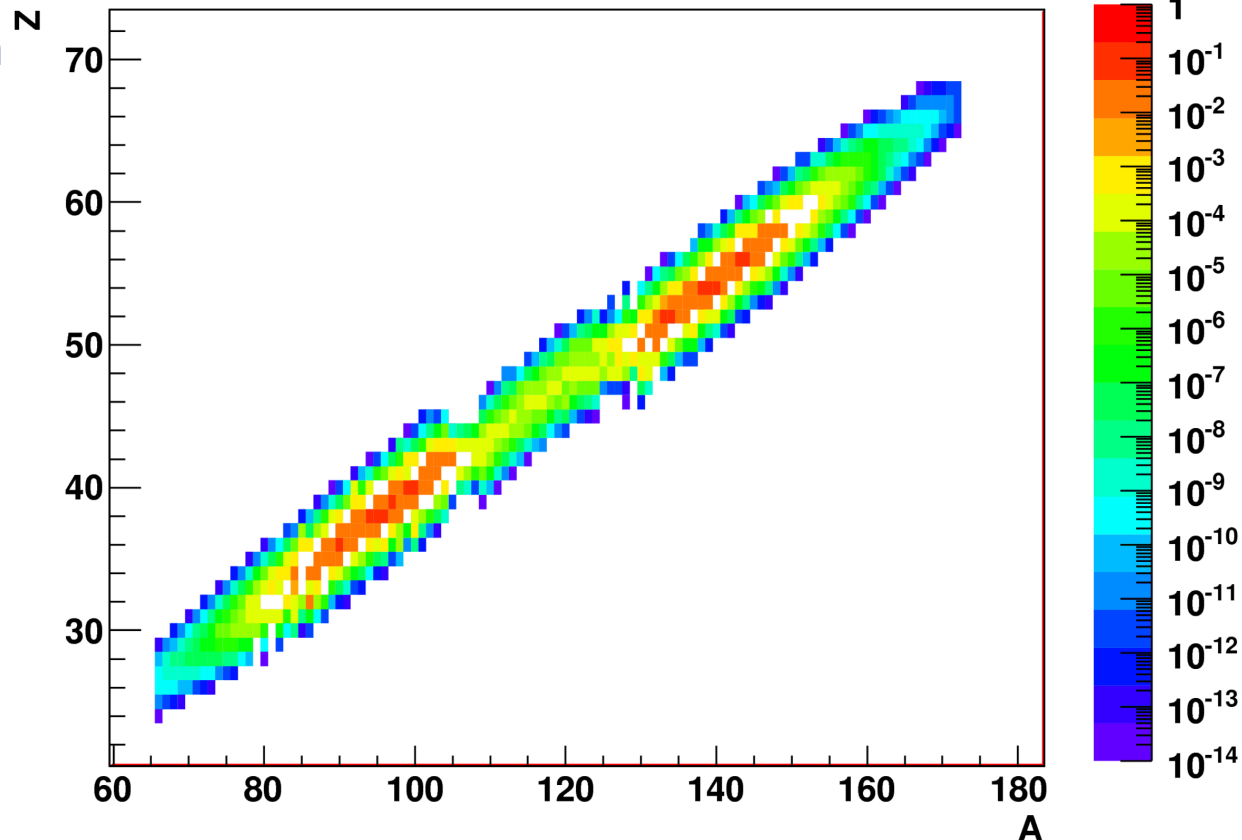
Fission fragment mass distribution

Distribution of fragment masses taken from neutron induced fission data for ^{235}U

All the neutrons emitted from the fragments are boosted back into the lab frame

Ratios are then formed at 90 degrees using simulated detectors both in and out of the plane of polarization

^{235}U fission fragment masses and relative yields from NNDC



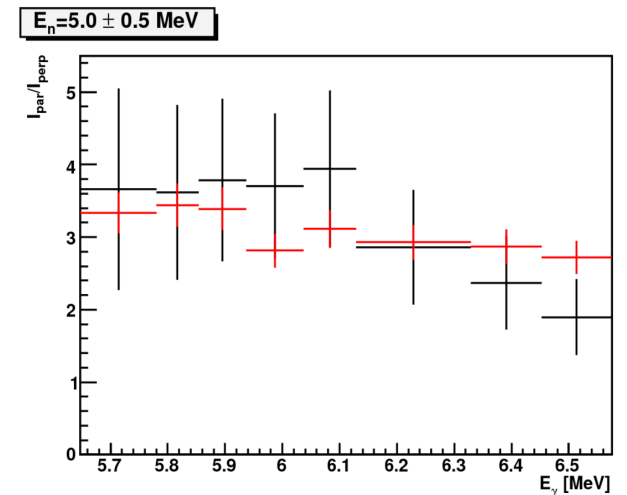
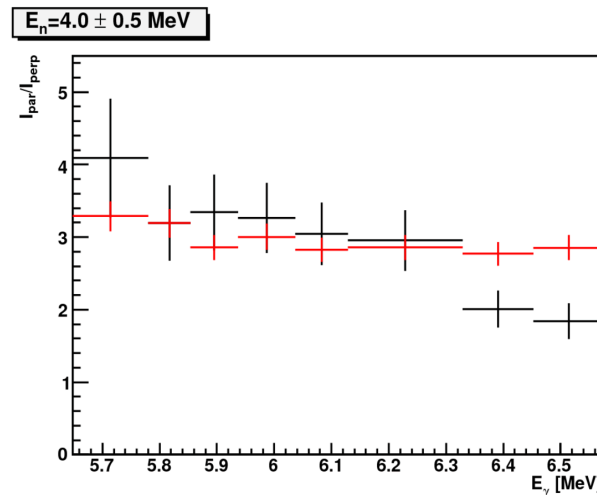
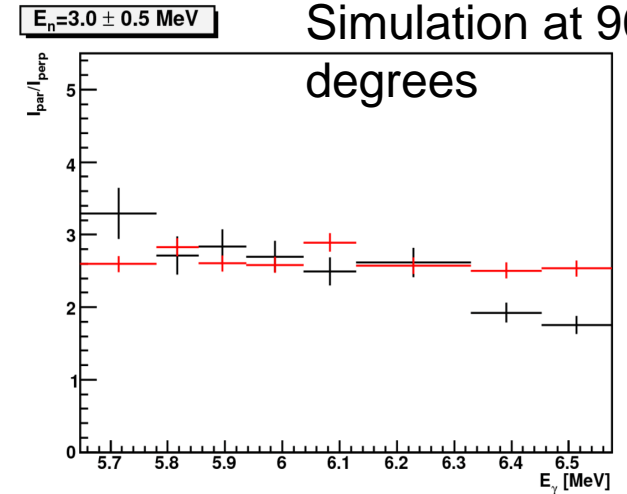
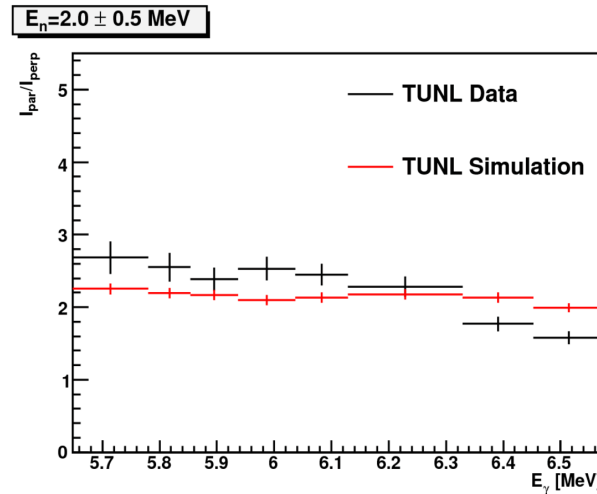
Simulation Results for ^{238}U

- Both trends as a function of incident γ -ray energy and outgoing neutron energy are recreated by the simulation

- Simulation tends to under-predict at low and over-predict at higher γ -ray energies

- Rabotnov data taken using a brems. beam

Data and Simulation at 90 degrees



Conclusion

I_{par}/I_{perp} has been **measured** for ^{238}U with $E_\gamma=5.7$ to 6.5 MeV

The results **agree well** with a new simulation based upon previously measured **unpolarized** angular distributions of fission fragments along with the assumption of dipole plus quadrupole excitations

Higher statistics data have been taken on ^{238}U and ^{235}U . Whereas values near 3.0 are found for ^{238}U , ***the results for highly enriched ^{235}U are consistent with 1.0.*** This factor of 3 difference could be a very useful tool for identifying enriched Uranium.